Synchronous Sampling Sideband Orders from Helical Planetary Gear Sets

Chad Edward Fair

Thesis submitted to the Faculty of the
Virginia Polytechnic Institute and State University
in partial fulfillment of the requirements for the degree of

MASTER OF SCIENCE
in
Mechanical Engineering

Alfred L. Wicks, Chair
Charles F. Reinholtz
William R. Kelley

August 3, 1998
Blacksburg, Virginia

Keywords: Synchronous, Sidebands, Vector, Averaging, Planetary, Gear, DAQ

Synchronous Sampling Sideband Orders from Helical Planetary Gear Sets

Chad Edward Fair

(ABSTRACT)

The sideband phenomenon is a common but obscure characteristic of the Rotary Dynamics field. In the automotive industry these sidebands have been found to produce a poor sound quality, resulting in customer dissatisfaction and warranty returns. In the interest of continued product improvement, research and development must resolve uncertainties in the current design methods. Qualitative relationships between the sideband characteristics and design parameters have developed in recent years, but the quantitative goal hasn't been achieved.

A Synchronous Sampling (SS) data acquisition system is applied to a helical planetary gear set to improve the understanding of the sideband characteristics and enhance the design process. An optical encoder, a component of the SS system, mechanically locked to the rotating system controls the A/D converter to sample at constant shaft angle increments. The phase-locked nature of SS allows the use of vector averaging to significantly lower the noise floor and improve the representation of the order domain.

In this work, the advantages of using a SS system with vector averaging capabilities are compared to the disadvantages of using a fixed sampling (FS) system. Utilizing the SS tool, this work also illustrates the influences of loading styles and values and speed on a gearmesh and its dominant sideband orders. Inspection of these influences suggests an opportunity for future work.

Acknowledgements

I would like to express my appreciation to Dr. Alfred L. Wicks, Dr. Charles F. Reinholtz, and Mr. William Kelley for their time serving on my committee. Special thanks go out to Mr. William Kelley and the Powertrain Systems division of Borg Warner Automotive for sponsoring this project.

I would like to dedicate this work and so much more to my parents Herbert and Linda Fair.

Table of Contents

List of Figures

List of Tables

Chapter 1. Introduction

1.1 Prelude

Today's high demand for automotive quality in the Sport Utility Vehicle (SUV) market as well as governmental noise requirements have motivated more stringent Noise and Vibration Harshness (NVH) standards. These standards were developed to lower or eliminate annoying sounds and customer dissatisfaction. The NVH category has one of the largest percentages of product warranty returns. Consumer pressure for higher quality at equal or lower consumer expense creates a waterfall effect. The automobile manufacturers require more from their component suppliers, who in turn demand more from their suppliers.

The powertrain in an automobile is a major noise source. SUVs commonly have a transfer case (Fig. 1.1.1) that is attached to the rear of the transmission and to the front and rear axles through propeller shafts (Fig. 1.1.2). The transfer case manages the power level and the direction that it flows to the wheels.

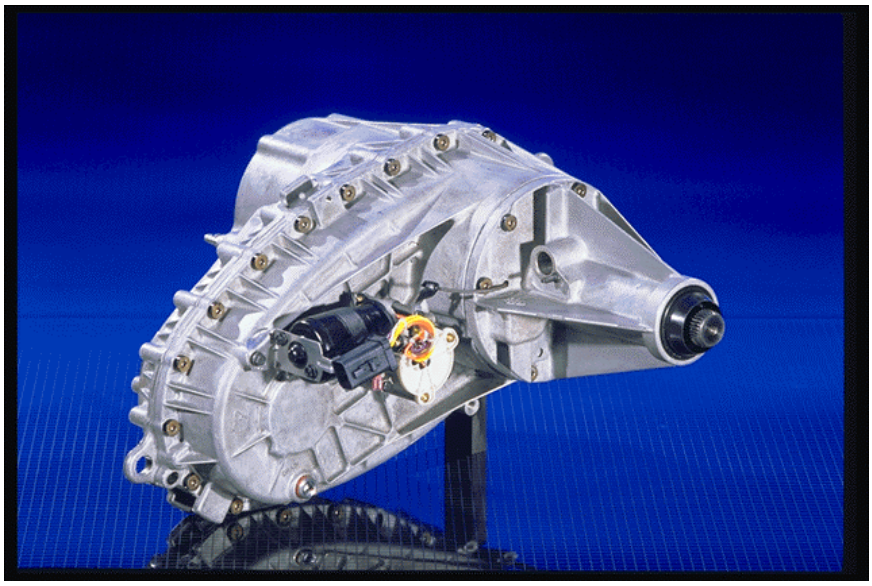

Figure 1.1.1. SUV Transfer Case Example – Photo
Example of SUV transfer case from the rear view, rear propeller shaft connection. (Photo Courtesy of *Borg Warner Automotive - Powertrain Systems*, Sterling Heights, MI)

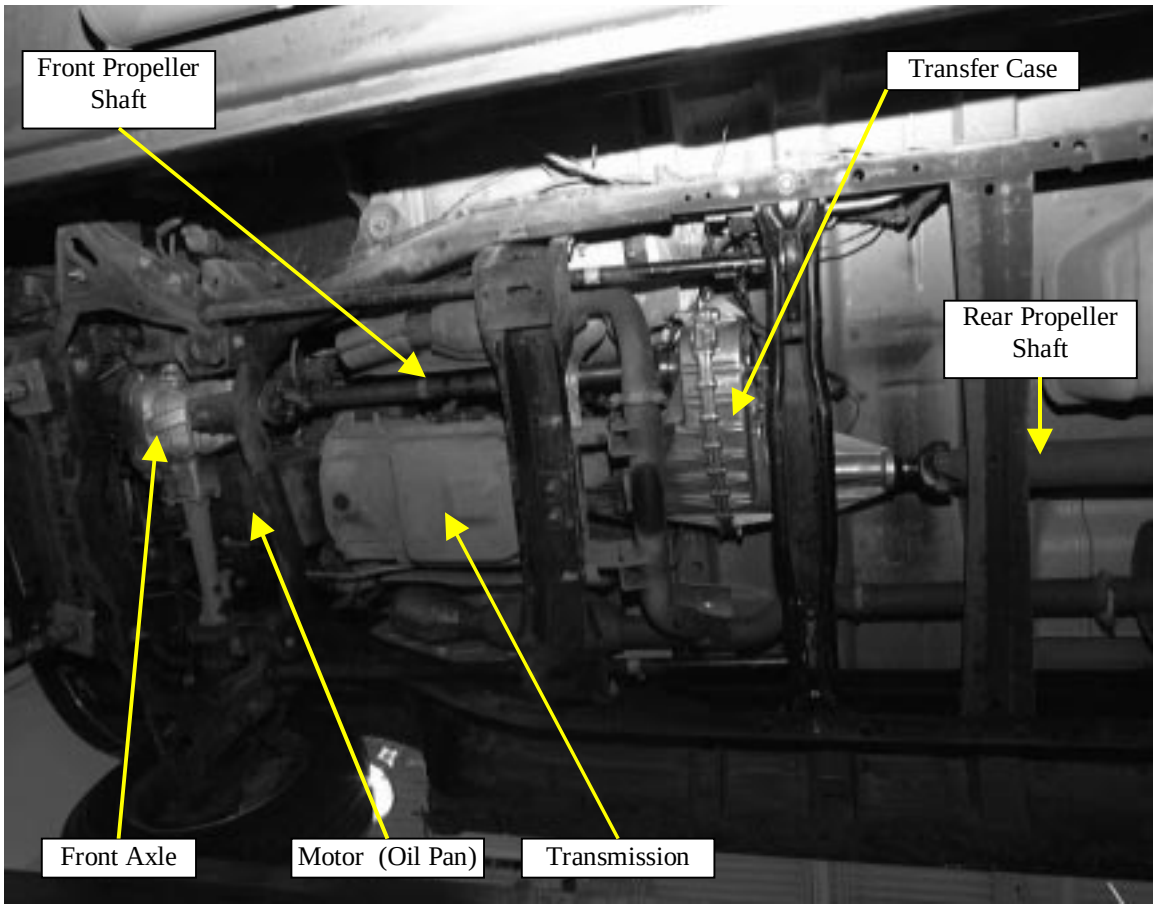

Figure 1.1.2. F150 Undercarriage – General Powertrain
The magnesium transfer case is bolted to the rear of the transmission with output propeller shafts running to the front and rear axles (front axle only shown). (Photo Courtesy of *Borg Warner Automotive - Powertrain Systems*, Sterling Heights, MI)

The location of the transfer case behind the transmission subjects it to the high torsional loads of the motor multiplied by the transmission gear reductions. Higher input energy from the motor increases the vibration and acoustic levels and the powertrain frequency contribution to the overall noise spectrum.

Transfer cases and transmissions commonly use planetary gear sets (Fig. 1.1.3) as an energy dense design to manage the torque and speed of the system. The planetary gear set increases the output torque while reducing the output speed by a factor of the mechanical advantage or gear set ratio.

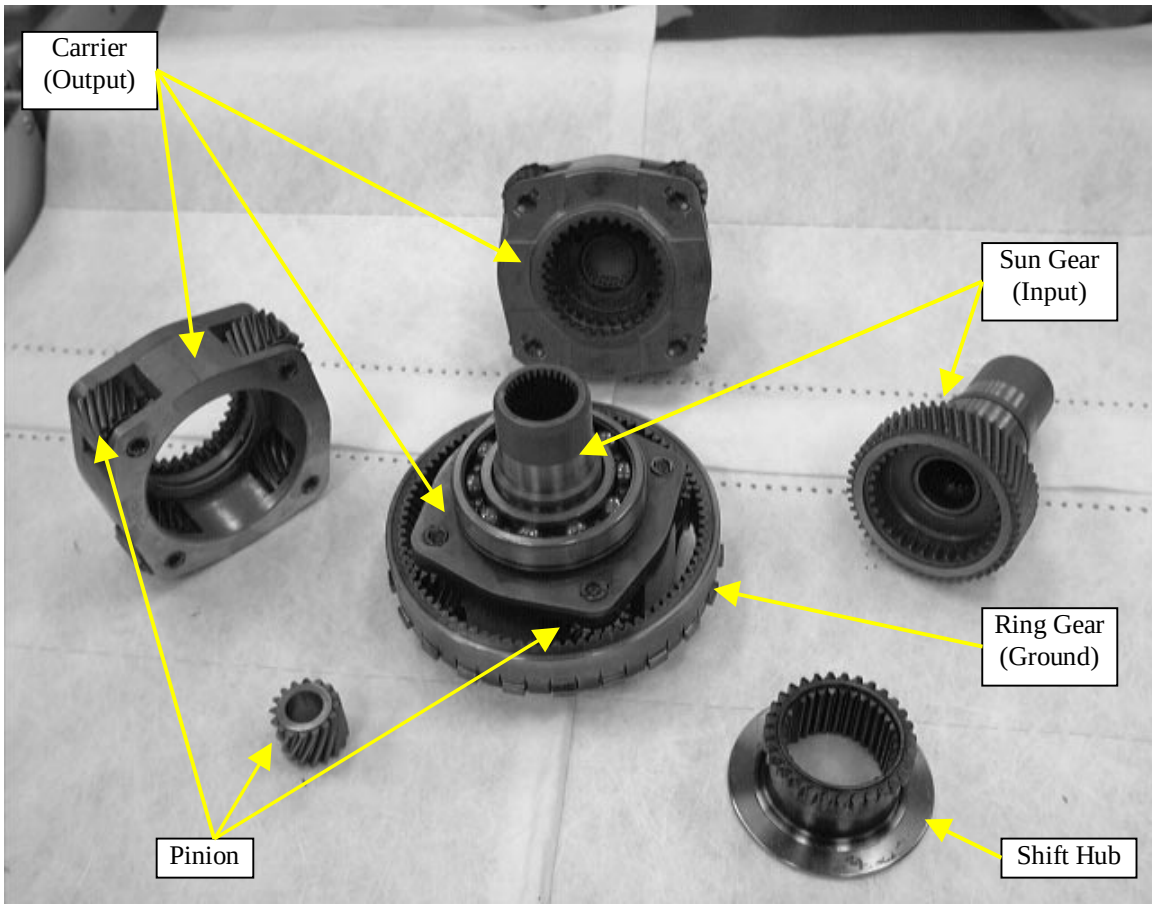

Figure 1.1.3. Planetary Gear Set – Components and Sub-Assemblies
The center object is the planetary gear set which consists of the input sun gear (right), four pinions or planets (bottom left), and the carrier or arm (sub-assembly with 4 pinions - left), and the ring gear. A planetary sub-assembly (minus ring gear – top) and shifting coupling (bottom right) are also shown. (Photo Courtesy of *Borg Warner Automotive - Powertrain Systems*, Sterling Heights, MI)

The speed and torque differences of the gear set produce two main vibratory signals. The gear-tooth-pass or gearmesh frequencies of these signals are related to the number of teeth and the relative rotating speed of the gears. They represent multiples of the rotating speed (orders) or cycles per rotation instead of the common cycles per time (Hz).

These signature orders also have adjacent order components called sidebands that typically produce a poor sound quality. The origins of the sidebands have yet to be defined in relation to specific gear design variables. General relationships are published that show relative changes in the vibration or acoustic levels on complex gear set systems. The ability to design and predict the sideband characteristics has not

been established. Sideband prediction is a deficient component of the gear design process, and it requires improvement.

The excitation of the gearmesh and sideband orders at constant shaft angles requires the data acquisition (DAQ) system to sample accordingly. The analog output signals from accelerometers or microphones must be digitally converted at these shaft angle positions. If the rotating speed is held constant, the fixed shaft angles will coincide with fixed time increments, and the analog-to-digital conversion (sampling) will acquire data at constant shaft angles (Synchronous Sampling) with a common fixed time sampling frequency (Fixed Sampling). A Fast Fourier Transform converts this data directly into the order domain.

Typically, the transfer case accelerates throughout an operational speed range consisting of multiple resonant (resonant frequencies) and synchronous (orders) vibratory signals. An Order Tracking (OT) analysis follows the orders as their frequencies vary with the shaft speed. In an OT analysis with a common Fixed Sampling system, the gearmesh order becomes a non-stationary signal due to the variation in the shaft angles and the constant time increments. As this discrepancy increases with greater speed variations leakage errors inflate within the signal.

With sampling speed advancements in the data acquisition hardware for fixed sampling frequencies, experimentalists abandoned the more expensive and slower, phase-locked loop design of the former SS system. Although great advantages were achieved with sampling speed, the data acquisition system is now constrained to sample at fixed time intervals. This limitation necessitates the use of additional Digital Signal Processing (DSP) to minimize the leakage error created from the temporal and geometric discrepancy. Computed Order Tracking (COT), a DSP method, interpolates these fixed sampled data points and the corresponding shaft angles of interest. An oversampling of the vibratory signals creates a finer temporal resolution, which improves this

interpolation process. The oversampling of the COT requires a higher sampling frequency, more volatile memory, and more hard drive space. Although the COT reduces the leakage error, the interpolation process inherently adds estimating error, resulting in phase-noise. With this added phase-noise, the COT configures the data into a pseudo-synchronous format, which may lead to misinterpretations.

A Synchronous Sampling DAQ system removes the phase-noise associated with estimating error. The SS data acquisition system used in this research utilizes the output signal from a digital, optical encoder as an external sample clock. This encoder outputs a square wave signal consisting of 1024 pules-per-revolution (p/rev) or one pulse every 0.35 degrees. Mechanically locking this encoder to an output shaft, the digital clock signal is synchronized with the rotating speed. The DAQ system now samples the analog input signals at constant shaft angle increments independent of any shaft speed variations. The direct transformation of these data blocks to the order domain eliminates the phase-noise caused by the estimating error of the COT method.

Typical to the automotive industry, powertrain components like transfer cases are ramped up or down throughout an operational speed range. There are benefits to observing the vibratory signals throughout this acceleration. In contrast, the sampling performed in this research is conducted under a steady state speed. This condition allows for the use of a fixed anti-alias filter and extensive averaging to enhance the signal-to-noise ratio. By synchronizing the data, the gearmesh orders are phase-locked to the beginning of each data block. This phase-locked approach benefits from the application of vector averaging. Vector averaging significantly reduces the noise floor below the Root-Mean-Square (RMS) averaged noise floor. With this lower noise floor, the improved order domain representation unveils the characteristics of the gearmesh and sideband orders.

A comparison between the SS and COT methods with the application of both the RMS and vector averaging schemes reveals the SS vector averaging combination as an improvement in the DAQ system of rotating machines. Applying this combination, further inspection of the influences of input load and speed on a gearmesh and its sideband orders reveals evidence that future work using this method of sampling is warranted.

1.2 Literature Review

Increases in microprocessor and memory speed inspired the implementation of Ron Potter's COT method in 1990[1]. Potter's technique acquires data with a fixed sampling frequency and a fixed anti-aliasing filter. Additionally, an interpolation filter resamples this data within the software to relate sampling times with shaft positions. The COT[2,3] competed with the phase-locked loop design of the former SS system. The tracking synthesizer and filters of this former system exhibited delays and phase noise under rapid changes in shaft speed. The COT was marketed as a reduction in size and cost without these errors. However, Fyfe's simulation of the COT revealed a modeling error[4].

Fyfe's simulation of the COT method evaluated key processing issues. This method hinges on the sampling rate of the so-called keyphasor pulse. The sampling rate requirement was found to be at least four times the frequency of the highest order of interest. To remove the smearing effects from the system, sample rates of 250 Hz, 1 kHz, 5 kHz, and 50 kHz were implemented to 1st, 4th, and 2.5 orders for a 200-

[1] W. Potter 1990 *Tracking and Resampling Method and Apparatus for Monitoring the Performance of Rotary Machines*. Arlington: United States Patent # 4,912,661.

[2] Potter, Ron. "A New Order Tracking Method for Rotating Machinery." Sound and Vibration Sept. 1990: 30-34.

[3] Potter, Ron, and Mike Gribler. "Computed Order Tracking Obsolete Older Methods." Proc. of the *1989 Noise and Vibration conference*, SAE Technical Paper Series (891131).

[4] Fyfe, K. R. and E. D. S. Munck. "Analysis of Computed Order Tracking." Journal of Mechanical Systems and Signal Processing 11(1997): 187-205.

1000 rpm ramp at 100 RPM increments. The highest order of interest (4^{th}) corresponds to an oversampling by a minimum of 4, 14, 71, and 714 with respect to these sample rates. This oversampling is well above the 2-time requirement of Shannon's Sampling Theorem. With these small orders, the magnitude values still held true for all cases, but the signal-to-noise ratio decreased an order of magnitude with a decreasing sample rate.

Fyfe investigated the effects on the linear acceleration assumption. Irregular shaped peaks and the highest noise floor occurred with the application of a non-linear acceleration at the higher 50 kHz sample rate. Even at this sample rate, this effect was mentioned as possibly masking bearing default sidebands.

Fyfe pointed out that the linear interpolation methods inherently incorporate error. Modeling with a piecewise cubic interpolation decreased the noise floor by an order of magnitude, but it was extremely sensitive to the calculated coefficients. An improvement of an additional order of magnitude was achieved with the implementation of a blockwise cubic spline.

Bandhopadhyay applied an optimized integration scheme to the Fixed Frequency (FF) method[5]. The traditional Fixed Frequency method exhibited smearing and leakage errors of the ordered content for variable speeds. The extended time requirement of a finer resolution increased this smearing error as the orders variation increased. This scheme integrated over a bandwidth centered on an order of interest. This integration scheme is limited to well separate orders. As in the case of sidebands, the integration is unable to distinguish between the leakage error and the sideband content.

Bandhopadhyay compared this FF method, the COT, the traditional SS, and Kalman filtering methods. For a 6-cylinder engine,

[5] Bandhopadhyay, D. K., David Griffiths. "Methods for Analyzing Order Spectra." Reprint from *Proceedings of the 1995 Noise and Vibration conference,* SAE Technical Paper Series (951273).

these methods were applied during an operational speed range of 1500-3000 RPM for both 2 and 17 Hz/s 1st order slew rates. The main discrepancy originated from the presentation of the systems (i.e. the phase-locked loop design of the former SS system references the initial RPM of a data block, but the COT references the average of the RPM range.)

Leuridan implements Kalman filtering into Noise and Vibration Harshness (NVH) evaluation of automotive drivelines. This narrow band pass digital filter was used to track a specific waveform within multiple harmonic time signals[6,7]. The slew rate limitation must be less than the sampling frequency divided by twice the acquisition time for a 1 Hz resolution. The speed signal must be sampled at a high rate and resampled (i.e. cubic spline) to acquire the arrival times and relate the signal to the order domain.

1.3 Scope

Sidebands produced from planetary gear sets can cause structural vibration and acoustic problems. Understanding the behavior of a sideband is crucial to determining the possible design considerations necessary to eliminate or advantageously position them. In addition, advancements must be made to resolve uncertainties in the current gear design methods.

This research entails the data acquisition and signal processing aspects of experimental rotary dynamic research. Specific emphasis is placed on the gearmesh and sideband orders of a helical planetary gear set. The vibration and acoustic specimen studied is the planetary gear set from a SUV, two-speed transfer case. The transfer case is tested

[6] Leuridan, Jan, Gary E. Kopp, Nasser Moshrefi, and Harvard Vold. "High Resolution Order Tracking Using Kalman Tracking Filters – Theory and Applications" Reprint from *Proceedings of the 1995 Noise and Vibration conference,* SAE Technical Paper Series (951332).

[7] LMS International. LMS CADA-X Test Monitor Manual. Rev 3.4. Leuven, Belgium: LMS International, 1996.

within a hemi-anechoic chamber (reflective floor surface). The base test configuration consists of the transfer case in the low-range position at an input speed of 3000 RPM with (800 in-lbs.) loads applied to both front and rear outputs. The acceleration and the Sound Pressure Level (SPL) are measured from an accelerometer mounted on the case near the input and a microphone hanging five feet above the accelerometer.

As the primary portion of this study, a SS DAQ system is developed to analyze the rotary dynamic system of a transfer case. This system uses a digital optical encoder mechanically attached to the rear output of the transfer case by a cog/belt system. The 1024 p/rev output signal of the encoder synchronizes the DAQ system with the mechanical vibrations of the transfer case. A comparison of this SS and the COT systems determine the influences of phase-noise created from COT's interpolations. A block averaging comparison (97 averages) determines the discrepancies between the RMS and vector averaging techniques on uncorrelated data.

The secondary portion of this research illustrates the implementation of the above Synchronous Sampling technique on the gear set parameters. The loading effects of the gear set are shown from measurements taken at five different loads in low range at a constant input speed of 3000 RPM. These loads are applied individually and simultaneously to the rear and front outputs. Additionally, an OT analysis illustrates the gear set parameters at different shaft speeds. The transfer case increases input speed in steps (100-RPM increments) ranging from 1000 to 3000 RPM under a constant load (800 in-lbs.) on both outputs. With the use of block vector averaging (50 averages) at each step, the gear set orders illustrate general trends with a significantly reduced noise floor.

Results containing gearmesh and sideband orders have been presented with order plots. Conclusions and suggestions for future research have also been offered.

Chapter 2. Gear Dynamic Overview

2.1 Gearing Introduction

Gears are common and versatile torque transmitters. Designers have struggled with gear acoustics for many years. The mass production of the various gear styles used in the automotive industry has created the feeling that is expressed in this quote from a paper presented at the American Gear Manufacturing Association (AGMA) conference:

> *...every gear is a quiet gear until it is made to run with another; then the gear set makes noise whenever it is operated.*[8]

Today, engineers still seek advancements in the vibration and acoustic design of gears. The following discussion of the basics of gear nomenclature, dynamics, and acoustics will show the underlying benefit of the Synchronous Sampling process.

2.2 Gear Pairs

The term "gears" encompasses both components when generally speaking about two meshing gears. When specifically describing each, the term "gear" is used for the larger diameter component while the term "pinion" is used for the smaller component. Mating gears common to automotive powertrains are designed with an *involute* tooth profile to maintain a constant angular velocity ratio (input/output angular velocities). The involute design maintains conjugacy without close shaft position tolerances. Conjugate profiles are designed to follow the Fundamental Law of Gearing: "for a pair of gears to transmit a constant angular velocity ratio, the shape of their contacting profiles must be such that the common normal passes through a fixed point on the line of

[8] Jones, Evan, and W. Route. "Noise Control in Automobile Helical Gears: Part I, Design Considerations in Gear Noise Control." American Gear Manufacturers Association 47th Annual Meeting, Hot Springs, VA 2-5 Jun. 1963.

centers."[9] This law of gear design is based on Kennedy's Theorem of Three Centers: "The three instantaneous centers of three bodies moving relative to one another must lie along a straight line."

Standard gears contain a common number of teeth in relationship to their diameter. When dimensioning with English units, the pitch and the Diametral pitch are represented as p (Eq. 2.2.1) and P (Eq. 2.2.2) respectively.

$$p = \frac{\pi d}{N} = \frac{\pi d_g}{N_g} = \frac{\pi d_p}{N_p} \tag{2.2.1}$$

$$P = \frac{N}{d} \tag{2.2.2}$$

N is the number of teeth on the gear, and d represents the pitch diameter. The module, m (Eq. 2.2.3), is used with SI units, and it represents the inverse of P or the number of millimeters of pitch diameter per tooth.

$$m = \frac{d}{N} \tag{2.2.3}$$

Using the gear as the driver (input) and the pinion as the driven (output), the Gear Set Ratio (GSR) or the Mechanical Advantage is determined from the ratio of the driver angular velocity to the driven angular velocity. A graphical Kinematics representation is shown in Fig. 2.2.1.

[9] Erdman, Arthur G., and George N. Sandor. Mechanism Design Analysis and Synthesis 2nd ed. New Jersey: Prentice Hall, 1991 Vol 1.

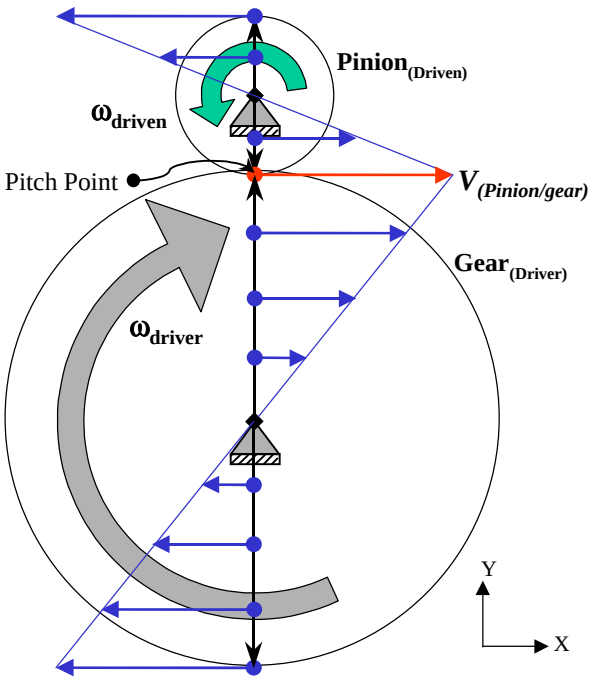

Figure 2.2.1. Gear Pair – Tangential Velocity Vector Schematic
The tangential velocity shown with vectors as a function of radial distance for two mating gears. The velocity at any point of the two gears is a linear relationship of each gear's rotating velocity, and radial distance from its center ground.

The contact point of the mating teeth must have the same tangential velocity vector. From this common velocity point, the angular velocity ratio is inversely related to the diameter or radius ratios (Eq. 2.2.4).

$$V_{(gear\ /\ pinion)_{cp}} = r_g\omega_g = -r_p\omega_p \qquad (2.2.4)$$

$$\frac{r_g}{r_p} = -\frac{\omega_p}{\omega_g}$$

The negative direction of the pinion's position vector creates the minus sign and represents the opposing rotating directions of the two gears. For the simplicity of the kinematics, Figure 2.2.1 shows the contact point along the line of centers called the pitch point, but it can be shown that the nature of the involute maintains a constant velocity ratio throughout the meshing cycle[10,11].

[10] Mabie, Hamilton H., and Charles F. Reinholtz. Mechanisms and Dynamics of Machinery. 4th Ed. New York: Wiley, 1987.

[11] Juvinall, Robert C., and Kurt M. Marshek. Fundamentals of Machine Component Design. 2nd Ed. New York: Wiley, 1991.

The inherent vibrating nature comes from the varying loads of the meshing teeth. Gear teeth are modeled as cantilever beams with a varying cross section. With respect to the tooth geometry, the contact point of the load moves up and down the tooth surface while the angle of the incident changes. As a tooth begins to mesh with a mating gear, the contact point starts at the base of the driver gear and at the tip of the driven pinion. The loads progress to the opposite ends of the profiles as the teeth finish their meshing cycle. With higher contact ratios, multiple teeth from each gear are meshing. A new tooth continues to increase the load that it carries as the previous tooth leaves contact and relieves its contribution. At the entering or leaving of teeth, the remaining tooth (teeth) has an immediate increase in load that creates loading pulses.

A series of these pulses created from each tooth produces a vibration throughout each rotation. The frequency of this signal is the product of the number of gear teeth and the rotating speed of the gear (Eq. 2.2.5).

$$f_{gm} = N * f_{shaft} = N * \omega_{shaft}\left(\frac{180}{\pi}\right) = N * \left(\frac{RPM}{60}\right) \tag{2.2.5}$$

The frequency signature is referred to as an order (N^{th}) of the fundamental rotating frequency. The rotating frequency of the shaft is the system's reference signature or fundamental order.

Two mating gears produce a single frequency. Using the pitch as an example, the ratio of gear teeth is directly related to the pitch diameter ratio.

$$\frac{N_g}{N_p} = \frac{d_g}{d_p} = \frac{r_g}{r_p}$$

The inverse relationship of the pitch diameters or gear tooth ratio with the rotational speed reveals the existence of only one gearmesh frequency.

$$\frac{\omega_p}{\omega_g} = \frac{N_g}{N_p} \Rightarrow N_g\omega_g = N_p\omega_p$$

$$f_{gm} = N_g \omega_g (\tfrac{180}{\pi}) = N_p \omega_p (\tfrac{180}{\pi})$$

2.3 Planetary Systems

The planetary gear set (Fig. 1.1.2) used within the transfer case is a more complicated case. A velocity vector schematic of the planetary system is illustrated in Figure 2.3.1.

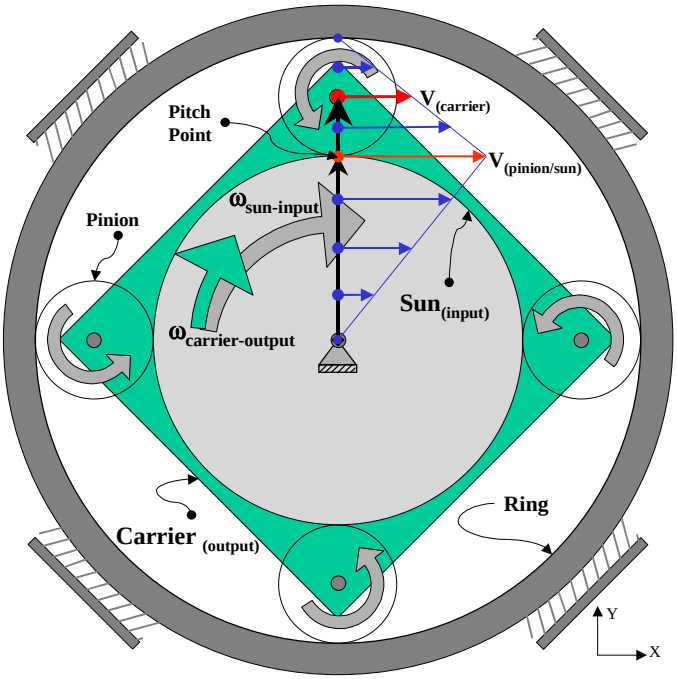

Figure 2.3.1. Planetary Gear Set – Velocity Vector Schematic
The absolute velocity is shown as vectors at radial distances away from the center of the sun gear (input).

This system utilizes the sun gear as the driver or input, and the carrier as the driven or output gear. The internal tooth ring gear is grounded to the transfer case housing which creates a rolling environment for the pinion gears. The carrier with needle bearings fixes the four pinions into position.

Eq. 2.3.1 employs the superposition of the rotation and translation components of the tangential velocity to the pinion/sun (2.3.2) and the pinion/ring (2.3.3) contact points.

$$V_{total} = V_{translation} + V_{rotation} \qquad (2.3.1)$$

$$V_{(pinion/sun)_{trans}} = 0$$

$$V_{(pinion/sun)_{rot}} = r_s\omega_s$$

$$V_{(pinion/sun)_{tot}} = V_{(pinion/sun)_{trans}} + V_{(pinion/sun)_{rot}} = r_s\omega_s \tag{2.3.2}$$

$$V_{(pinion/ring)_{trans}} = 0$$

$$V_{(pinion/ring)_{rot}} = 0$$

$$V_{(pinion/ring)_{tot}} = V_{(pinion/ring)_{trans}} + V_{(pinion/ring)_{rot}} = 0 \tag{2.3.3}$$

With the ring gear grounded and the sun gear pinned by a bearing, the pinion orbits about the sun gear and rolls along the ring gear. Unlike the pure rotation of the sun gear (Eq. 2.3.2), the rolling pinion contains both a translation and a rotation component (Fig. 2.3.2).

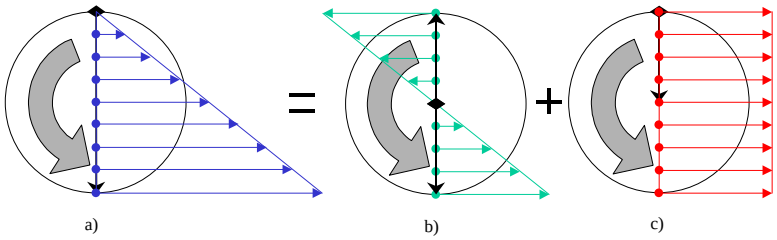

Figure 2.3.2. Planetary Pinion – Velocity Vector Schematic
The absolute velocity for a single pinion with respect to the gear set ground (ring gear). The total rolling aspect (a) of a pinion is illustrated along with the translation (b) and rotation (c) components.

$$\omega_{(pinion/ring)} = \frac{V_{(pinion/sun)_{cp}}}{d_p} \tag{2.3.4}$$

The pinion's angular velocity (Eq. 2.3.4) produces the rotational component at the tooth contact points according to Eq. 2.3.5.

$$V_{pinion_{rot}} = r_p\omega_{(pinion/ring)} = \frac{V_{(pinion/sun)_{cp}}}{2} \tag{2.3.5}$$

Since the rotation component is half of the total pinion/sun velocity, the remaining half is the translation component. The translation component is independent of the position on the pinion and is equivalent at any point on the pinion. The rotational component is a function of the pinion's radial distance.

$$V_{pinion_{trans}} = V_{(pinion-sun)_{tot}} - V_{(pinion-sun)_{rot}}$$

$$\left|V_{pinion_{rtrans}}\right| = \left|V_{(pinion/ring)_{rot}}\right| = \left|V_{(pinion/sun)_{rot}}\right|$$

$$V_{pinion_{tot}} = V_{pinion_{trans}} + V_{pinion_{rot}}$$

The total velocity of the pinion as depicted in Figure 2.3.1 & 2.3.2(a) is the summation of the translation and rotation components.

The gear set ratio (GSR) is the ratio of the input to output angular speed. Table 2.3.1 lists the number of teeth and diameters of each component. Applying these values into Eq. 2.3.6, the gear set has a mechanical advantage or GSR of 2.64:1.

Table 2.3.1. Gear Counts & Sizes

Gear	Diameter [mm]	Teeth	Normal Module	Helix Angle []
Sun	95.329	50	1.7500	23.383 – LH
Pinion	30.505	16	1.7500	23.383 – RH
Ring	156.340	82	1.7500	23.383 – RH
Carrier	62.917	NA	NA	NA

$$GSR = \frac{\omega_i}{\omega_o}$$

$$\omega = \frac{V}{r}$$

$$\frac{\omega_i}{\omega_o} = \frac{\left(\frac{V_{sun}}{r_s}\right)}{\left(\frac{V_{carrier}}{r_c}\right)} = \frac{\left(\frac{V_{sun}}{r_s}\right)}{\left(\frac{\left(\frac{V_{sun}}{2}\right)}{\left(r_s + r_p\right)}\right)} = \frac{2\left(r_s + r_p\right)}{r_s} = 2 + \frac{2r_p}{r_s}$$

$$r_r = r_s + 2r_p$$

$$GSR = \frac{\omega_i}{\omega_o} = 1 + \frac{r_r}{r_s} = 1 + \frac{N_r}{N_s} \qquad (2.3.6)$$

$$GSR = 1 + \frac{82}{50} = 2.64$$

The planetary gear set has two gearmesh frequencies pertaining to sun/pinion (Eq. 2.3.7 a,b) and pinion/ring (Eq. 2.3.7 c,d) mating gear teeth. The relative angular velocity of the rotating input and output components of the planetary gear set produce two sets of orders.

$$f_{gm(p/s)} = N_s * \left(\frac{RPM_i}{60}\right) \; ; \; f_{gm(p/s)} = N_s * \left(\frac{RPM_o * GSR}{60}\right) \qquad (2.3.7a,b)$$

$$f_{gm(p/r)} = N_r * \left(\frac{RPM_i}{60 * GSR} \right) \; ; \quad f_{gm(p/r)} = N_r * \left(\frac{RPMo}{60} \right) \qquad (2.3.7c,d)$$

Table 2.3.2. Gearmesh Orders

	Input Ref	Output Ref
Pinion/Ring	31.0606…	82
Pinion/Sun	50	132

By using the lower speed output shafts as the speed reference signal, the orders of the gear set are increased by a factor of the GSR. With this gear set, the planet/ring gearmesh order changes from a fraction to an integer, while the planet/sun gearmesh order remains an integer (Table 2.3.2). The signal processing significance of the integer orders will be discussed later in Chapter 3.

The above analysis was for one pinion. Each of the four pinions vibrates with the same frequency signal. The relative phase of each of these signals depends on the position of the tooth meshing cycle of one pinion relative to the others. The effects of adding two pinions with the same frequency and a 30° phase difference are simulated in Figure 2.3.3.

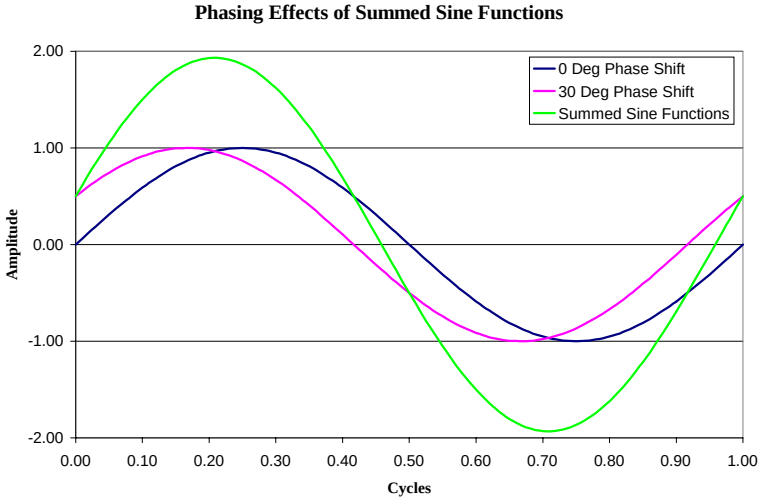

Figure 2.3.3. Phasing Effects of Summing Sinusoids
Phasing effects of adding two sine waves with amplitude of unity and a frequency of unity. The 30°-phase shift between them results in a single summed sine function with the same frequency, higher amplitude, and a phase angle equal to the phase difference.

The amplitude effect of the resultant sine wave is dependent on the degree of phase shift (Fig. 2.3.4). The multiplication factor produces an

amplification effect for phase difference between 0-120° and 240-360°, and an attenuation result for the values between 120-240° (Fig. 2.3.5)

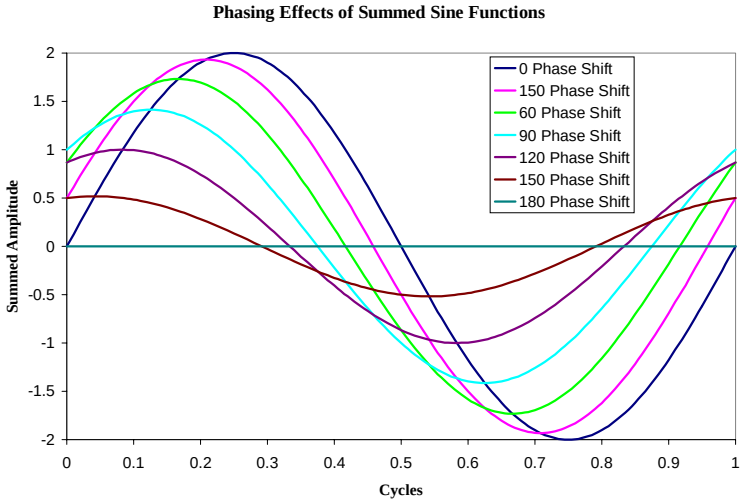

Figure 2.3.4. Phasing Effects of Summed Sinusoids – Various Phase Shifts Functions
Phasing effects of two similar sine functions with different phase shifts. The summed waves are amplified for a phase difference less then 120°, an equal amplitude at 120°, and the summed sine function is attenuated from 120° to 0 amplitude at 180°

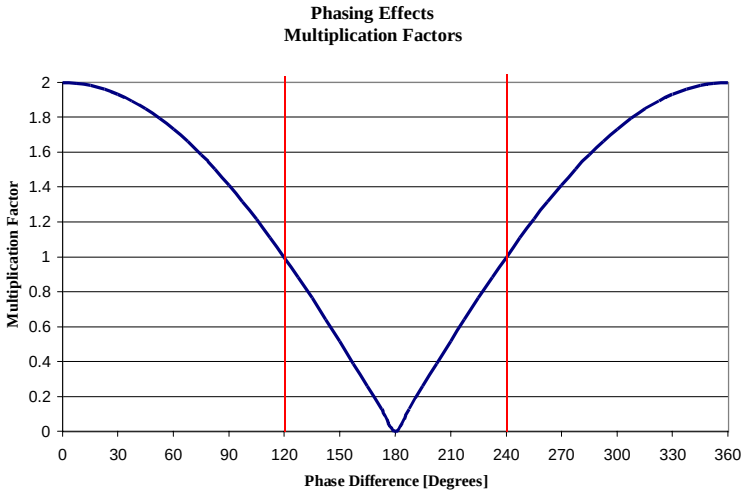

Figure 2.3.5. Phasing Effects of Summed Sinusoids – Multiplication Factors
The amplification and cancellation effects for two similar sine functions that have various phases. Any phase shift less than 120° or greater than 240° produces an amplification of the previous signals. The function is attenuated between the red lines.

Designers have deliberately placed the pinions out-of-phase with one another or counterphase them to minimize or negate the vibration.[12]

[12] Hardy, Alex. The Cause of Gear Noise: The Theory Behind "Counterphasing". Detroit Transmission Division: General Motors Corporation. Detroit, MI: 1961.

Counterphasing of planets in a gear design is used to balance the simultaneous pinion tooth mesh loads. Noise levels have been reduced for helical planetary gear sets with the use of sequential planet phasing, but it is more noticeable in the spur gear configurations.[13]

Two similar acoustic functions that are radiating energy from different points will have various phase differences when summed at different places in space. Figure 2.3.6 illustrates the time signal of two sine functions with incremental phase differences. This also represents the amplitude at different distances along a standing wave.

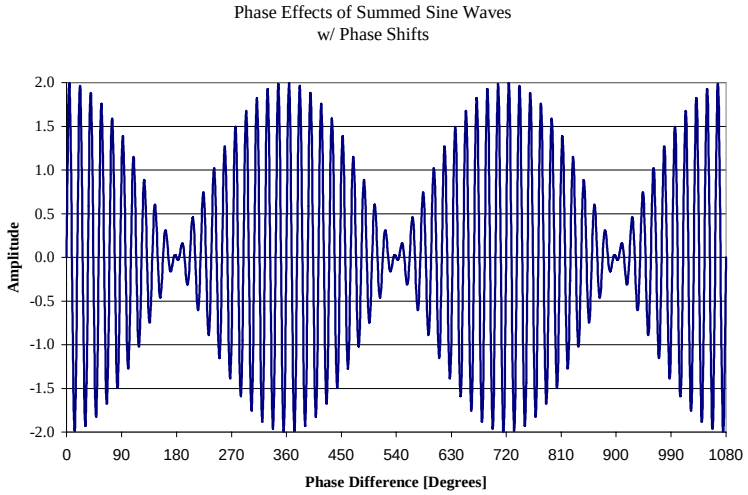

Figure 2.3.6. Phasing Effects of Summed Sine Waves – Changing Phase
Two Sine waves with the same frequency (1 Hz) and the same amplitude (unity) summed together with an increasing phase shift.

2.4 Analytical Sideband Modeling

Sidebands are orders found at the spectral lines next to the gearmesh orders. These sidebands are believed to originate from a transmission error found in the gear design and/or the manufacturing. The harmonic characteristics or just the presence of a sideband are perceived as a fatigued or low quality design. Unfortunately, a specific

[13] Platt, R. L., and R. D. Leopold. A Study on Helical Gear Planetary Effects on Transmission Noise. Proc. Of VDI Berichte NR. 1996.

gear error has yet to be related to specific sideband characteristics like spacing, asymmetry, and amplitude.

The models used by A K Dale[14] and Luo[15] are among the few published mathematical models used in an attempt to model the rotary dynamic sidebands. "The effects of the errors introduced into the gears at the various stages of manufacture are difficult to assess in terms of noise generation properties." These models come from design and signal processing techniques used in the Communications industry. The basic and common Amplitude Modulation is described along with the higher order Frequency and Complex Modulation models.

2.4.1 Amplitude Modulation

Two different load cases are applied to the Amplitude Modulation (AM) model. A cosine function is used to resemble the pinion/ring gearmesh frequency with the rear output or carrier angular velocity used as the carrier or fundamental gearmesh order. The modulating signal is also a cosine function with a first order frequency and an amplitude of unity. Although various characteristics could be applied, this simulation is an attempt to model the shaft runout common to rotating machinery.

Equation 2.4.1.1 shows the condensed and expanded forms of the AM model. The characteristics of the gearmesh frequency are independent of the modulating signal characteristics, but the sidebands are dependent on both signals.

[14] Dale, A K. "Gear Noise and the Sideband Phenomenon." Proc. of the American Society of Mechanical Engineers 1984 Design Engineering Technology Conference: 7 Oct., 1984, Cambridge, MA.

[15] Luo, M. F., and J. Mathew. "A Theoretical Analysis and Simulation of Amplitude Modulated Signal." Proc. of the Institution of Engineers Austrialia Vibration and Noise Conference: 18-20 Sept., 1990, Melbourne, Austrialia.

$$\begin{aligned} M(t) &= A_c(1 + A_1 Cos(\omega_1 t + \theta_1))Cos(\omega_c t + \theta_c) \\ &= A_c Cos(\omega_c t + \theta_c) \\ &+ \tfrac{1}{2} A_c A_1 Cos((\omega_c + \omega_1)t + \theta_1 + \theta_c) \\ &+ \tfrac{1}{2} A_c A_1 Cos((\omega_c - \omega_1)t + \theta_1 - \theta_c) \end{aligned} \qquad (2.4.1.1)$$

Figure 2.4.1.1 (a) illustrates the results of a computational simulation for a rpm step-up function in a waterfall plot. The amplitudes are independent of the rotating speed and constant throughout the various output rpm speeds. Figure 2.4.1.1 (b) shows a close view of the order content at a constant rpm. Depending on the desired modulating amplitude used as the input, the sidebands can surpass the fundamental gearmesh amplitude. The summations and differences of the carrier and modulating frequencies determine the frequencies or orders of the sidebands. These characteristics give the sidebands symmetric form about the gearmesh order.

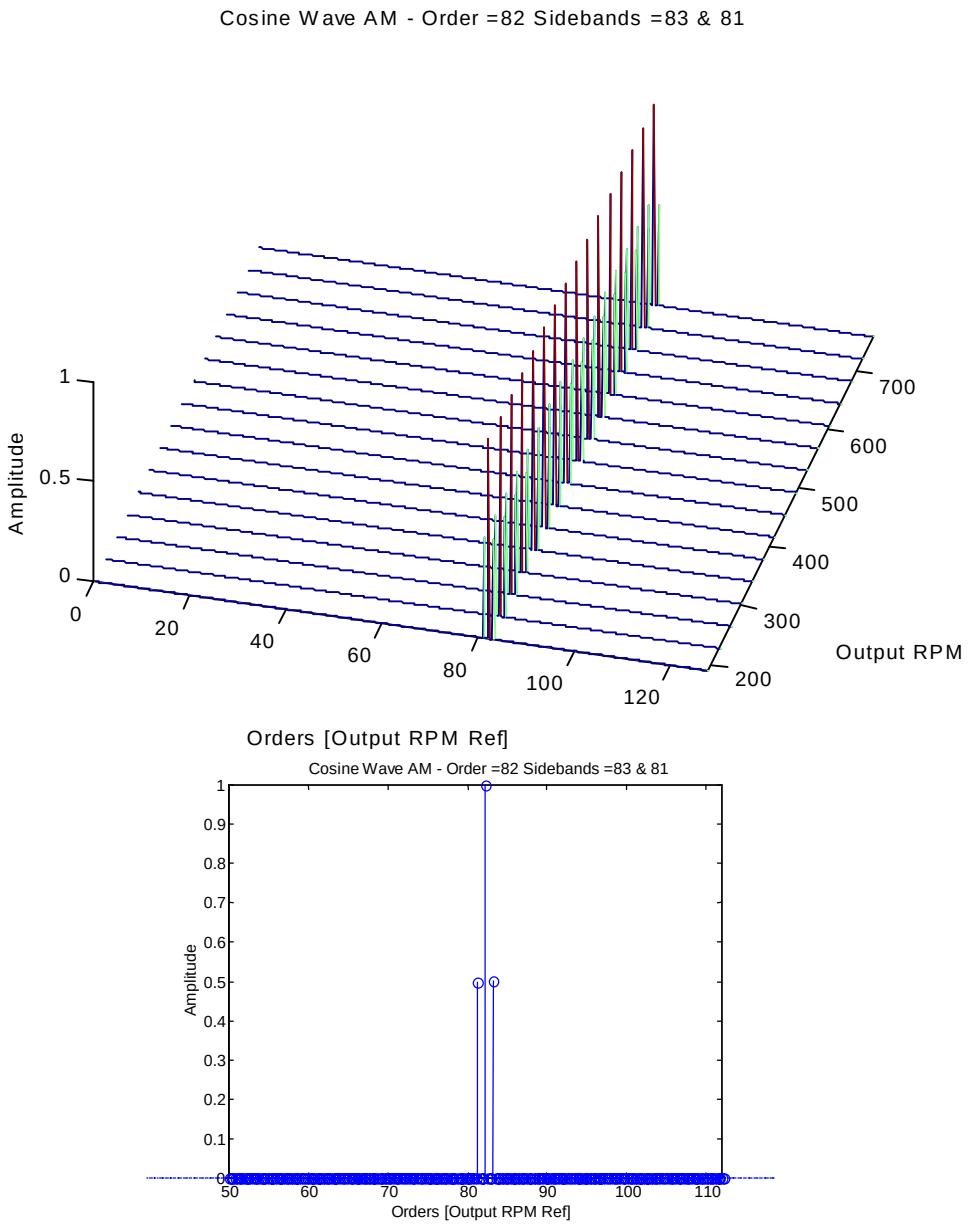

Figure 2.4.1.1. AM – Cosine Modulation
An 82nd gearmesh order with amplitude of 1 is modulated by a cosine with equal amplitude and a 1st order frequency. The AM model is displayed for a rpm step function in a waterfall plot (a) along with an order plot (b) with a close view for a constant rpm.

The difference should be noted between the summing of harmonic signals discussed in section 2.3 and the multiplication of the harmonic signals used with the AM model. The multiplication of the AM signals in the time domain relates to a convolution of the signals in the frequency

domain. The AM model creates three spectrum components while the summing effect only produces two frequency peaks.

As another input example, a square wave is used with the same amplitude and frequency as the previous modulating cosine function. This also results with an unaffected fundamental frequency. About the gearmesh order, there is an infinite set of symmetric sidebands that reside at all of the odd orders. The sideband amplitudes exponentially decay as the sideband orders separate further away from the gearmesh order. Figure 2.4.1.2 illustrates a waterfall plot for the same rpm step function and an order plot for a constant rpm.

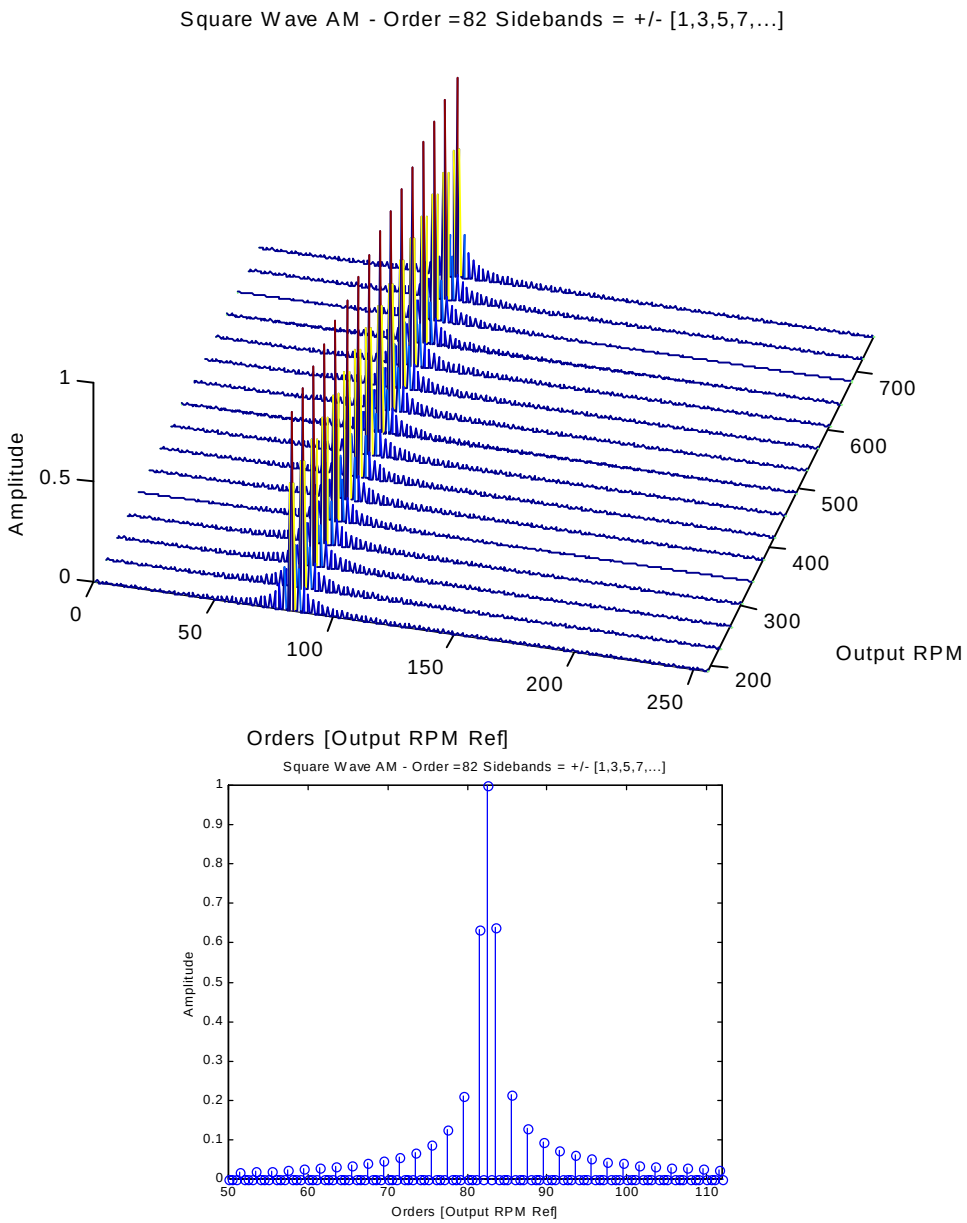

Figure 2.4.1.2. AM – Square Wave Modulation
An 82nd gearmesh order with amplitude of 1 is modulated by a square wave with equal amplitude and a 1st order frequency. The AM model is displayed for a rpm step function in a waterfall plot (a) along with an order plot (b) with a close view for a constant rpm. The sidebands are spaced at every odd order greater or lesser than the fundamental gearmesh.

2.4.2 Frequency Modulation

The amplitudes of a Frequency Modulation (FM) model are governed by Bessel functions of the 1st kind. Equation 2.4.2.1 represents two forms of the mathematical model. This Fourier Series represents an infinite ensemble of sidebands surrounding the fundamental frequency. In automotive powertrains, the driving frequency (ω_c) along with the coupled modulating frequency (ω_2) increase with vehicle speed. The modulating depth (I) is the Bessel function's root, and it is inversely proportional to the vehicle's speed and will converge to zero. From Figure 2.4.2.1, the fundamental frequency (m=0) is at unity while all of the sidebands are at zero at the origin. The maximum modulation amplitude, $\Delta\omega_c$, will determine the starting point on the curves, and the driving speed range (vehicle frequency range) will decide the convergence of I.

$$M(t) = A_c Cos(\omega_c t + \theta_c + \frac{\Delta\omega_c}{\omega_2} Sin(\omega_2 t + \theta_2)) \qquad (2.4.2.1a)$$

$$M(t) = A_c \sum_{m=-\infty}^{\infty} J_m(I) Cos(\omega_c t + \theta_c + m(\omega_2 t + \theta_2)) \qquad (2.4.2.1b)$$

$$I = \frac{\Delta\omega_c}{\omega_2} \qquad I \Rightarrow 0 \text{ As } \omega_2 \Rightarrow \infty$$

c – carrier frequency attributes; 2 – modulating frequency attributes

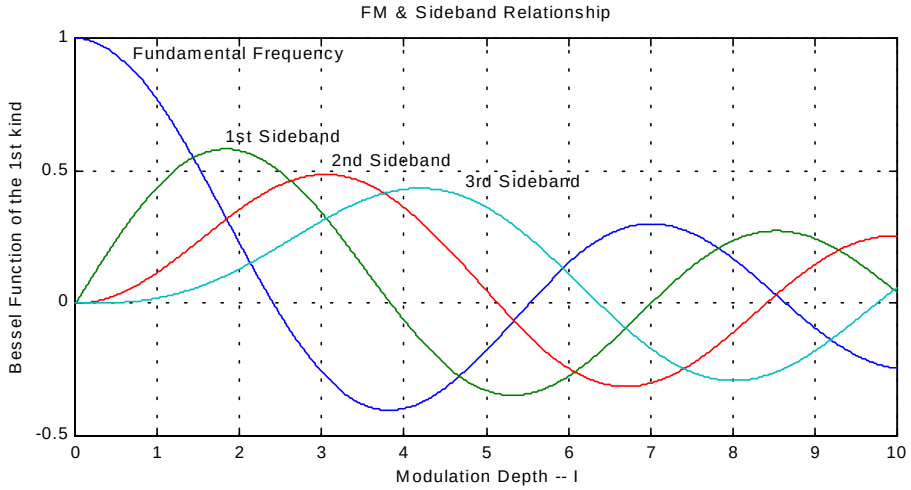

Figure 2.4.2.1. FM – Bessel Functions of the 1st Kind
The Bessel functions of the 1st kind control the amplitude of the FM fundamental gearmesh and its sideband orders.

Figure 2.4.2.2 illustrates the results of the FM computational analysis.

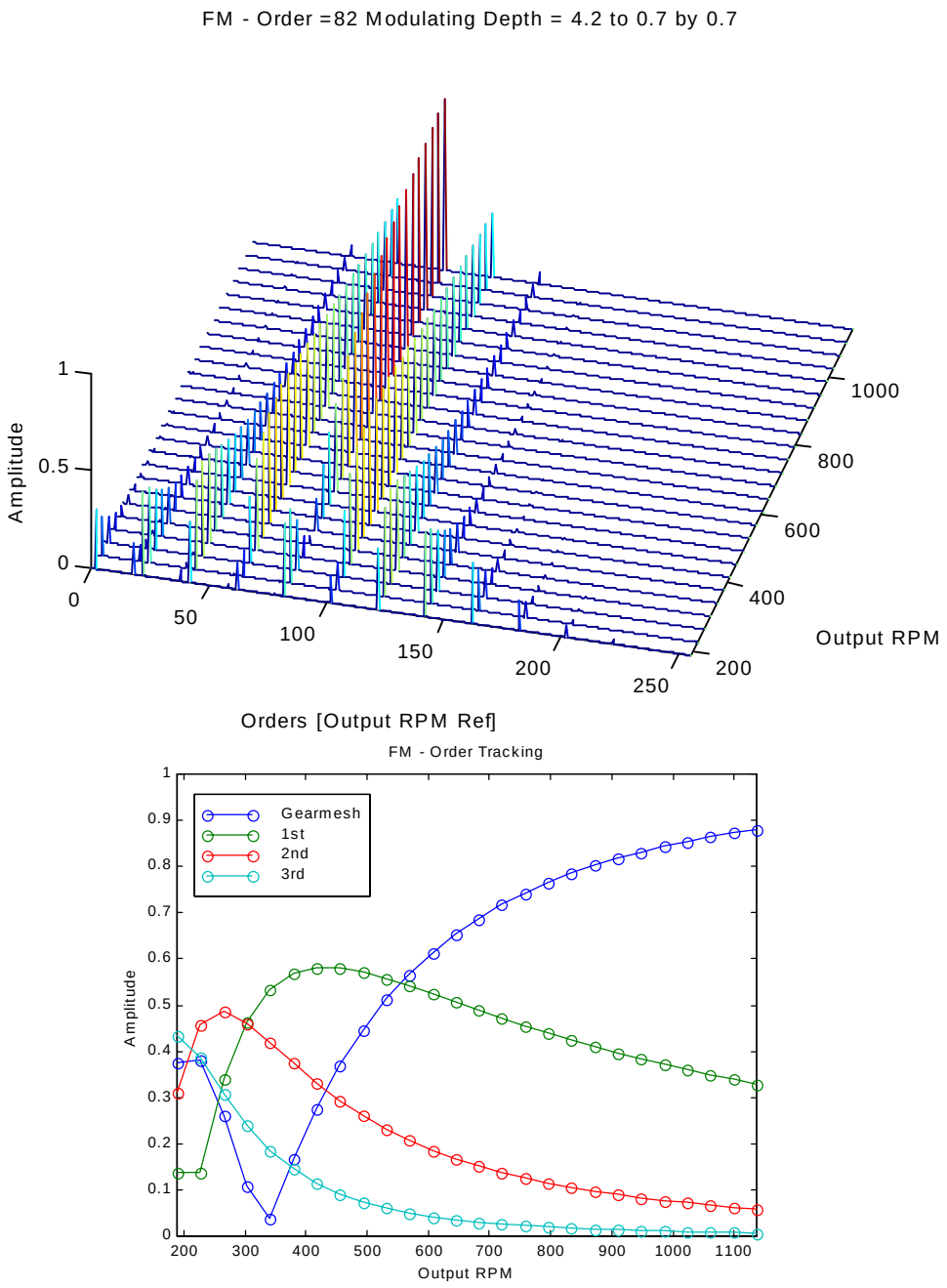

Figure 2.4.2.2. FM – Fundamental and Sidebands
An 82nd gearmesh order has amplitude of 1 with a 20th modulating cosine order. The waterfall plot (a) displays the frequency spacing and the amplitude variation for the rpm step up function. The order tracking plot (b) of the gearmesh and the first three sidebands resembles the Bessel functions of the 1st kind.

A modulating order of 20 with the maximum modulating amplitude of 700 produces a modulating depth of 4.2 back to 0.7 by steps of 0.7 for the rpm range. An order tracking plot (Fig. 2.4.2.2b) of the gearmesh order along with the first three sidebands agree with the Bessel function

plot (Fig. 2.4.2.1). As the modulation depth approaches the origin at a higher rpm, the fundamental gearmesh and sideband orders converge to unity and zero respectively. The rate of convergence increases as the order of the Bessel function or sideband increases. Although, the sidebands have dominant amplitude when fundamental order resembles the Bessel function at a node or approximately 330 RPM. Once again, the symmetry holds about the carrier order.

2.4.3 Complex Modulation

The Complex Modulation (CM) model is a higher order model that contains both the AM and FM models. The CM model contains an asymmetric frequency domain format, unlike both previous models. The mathematical model (Eq. 2.4.3.1) represents an example of a carrier frequency that is amplitude and frequency modulated by two different signals each. The first term contains the fundamental frequency and the FM portion of the sidebands. The following terms contain the AM portion of the sidebands. The asymmetric characteristic of typical gearmesh frequency spectrums comes from the inter-modulated products.

$$\begin{aligned} M(t) &= A_c \sum_{m=-\infty}^{\infty} \sum_{n=-\infty}^{\infty} J_m(I_1) J_n(I_2) Cos(\omega_c t + \theta_c + m(\omega_1 t + \theta_3) + n(\omega_2 t + \theta_4)) \\ &+ \tfrac{1}{2} A_1 Cos(\omega_c t + \theta_c + (m+1)\omega_1 t + m\theta_3 + \theta_1 + n(\omega_2 t + \theta_4)) \\ &+ \tfrac{1}{2} A_1 Cos(\omega_c t + \theta_c + (m-1)\omega_1 t + m\theta_3 - \theta_1 + n(\omega_2 t + \theta_4)) \\ &+ \tfrac{1}{2} A_2 Cos(\omega_c t + \theta_c + m(\omega_1 t + \theta_3) + (n+1)\omega_2 t + n\theta_4 + \theta_2) \\ &+ \tfrac{1}{2} A_2 Cos(\omega_c t + \theta_c + m(\omega_1 t + \theta_3) + (n-1)\omega_2 t + n\theta_4 - \theta_2) \end{aligned} \qquad (2.4.3.1)$$

A K Dale mentions the need for a “fine resolution order-locked analysis” to properly acquire experimental gear data. Such systems are discussed in Chapter 3 with the intent to improve the correlation between the experimental and design stages.

Chapter 3. Signal Processing of Rotary Dynamics

3.1 Rotary Dynamics and the Order Domain

Rotating machines contain rotating imbalances, gear tooth imperfections, and runout. These mechanical imperfections produce vibration signals associated with the number of cycles per revolution (orders) instead of per time (Hz). These synchronous signals represent excitations in a geometric coordinate system at constant shaft angles instead of a typical temporal coordinate system at constant time intervals. The conversion between the frequency and the order domain is a scalar multiplication or order of the reference shaft rotating speed. For the planetary gear set of the transfer case, these orders include the meshing cycles of the gear teeth. With an operating input speed range of 0-5000 RPM (0-84 Hz), the DAQ systems track the gearmesh orders as they change frequency. Most commercial DAQ packages contain a fixed time data acquisition board. The discrepancy between the hardware and the rotating dynamics require additional processing effort to correlate these signals. By properly acquiring the data at the appropriate shaft angles, these signals contain a simple and more direct relationship.

An Order Tracking (OT) analysis as applied to the Rotary Dynamics field follows the synchronous orders as their frequency changes with rotating speed. A Fixed Sampling (FS), common to commercial DAQ packages, continuously acquires data at fixed times independent of the shaft rotating speed. The Fixed Frequency (FF) and the Computed Order Tracking (COT) methods attempt to relate the acquisition time with the shaft speed. A speed signal from the rotating shaft is sampled along with the input channels to form this relationship. This relationship is the cornerstone of the FF and COT methods.

The FF method performs a Fast Fourier Transform directly to the temporal data block without any additional DSP. This method contains

leakage and smearing errors that attenuate the amplitudes of the synchronous content. The COT method acquires a large block of data at a relatively high sample rate or oversamples the orders in relation to their frequency. An additional interpolation and curve-fitting algorithm is implemented to resample the data block. This block of data is converted into a pseudo-synchronous format. This format attempts to remove the smearing error and reduces the leakage error, but it adds the interpolation and curve fitting error.

The Synchronous Sampling (SS) method performs an OT in a different way. With this method, the DAQ hardware collects data at known shaft angles independent of time. The hardware requires an external-sample-clock signal to track the rotating shaft speed and operate the (A/D) conversion. A Fast Fourier Transform directly transforms the data block into the order domain. This method removes the smearing and the estimate error associated with the methods mentioned above, but extra hardware is required.

The advancements of the FS DAQ systems over the past ten years inspired the development of the COT method. The appealing nature of the COT's reduced hardware has drawn a lot of attention, and most experimentalists have abandoned the SS method due to its expense. The SS method is revisited here to assess the errors contained within the COT.

3.2 Fixed Sampling

Most commercial data acquisition packages limit their acquisition capabilities to a fixed sampling frequency. By fixing the slow anti-alias filter, the Analog-to-Digital conversion doesn't have to wait for the filter to settle, which allows a higher performance speed. Although the sampling speeds of the DAQ boards have increased, signal processing techniques have also grown in complexity to compensate for the FS limitation. FS can advantageously acquire the data with minimal hardware components

like a data recorder and then postprocess it in various ways and at convenient times, but the extra modeling and estimations add extra error.

3.2.1 Fixed Frequency

To understand the application of the FF method to an OT analysis, the FS theory is described. The analyst commonly chooses the bandwidth or maximum frequency and the resolution, and the remaining dependent values are performed behind the scenes. Corresponding to the maximum frequency, the analog-to-digital (A/D) computer board then sets the anti-aliasing cut-off frequency and the sampling frequency to a multiple of 1.28 and 2.56 respectively. The resolution setting or the number of spectral lines determines the data blocksize or memory requirement. The number of spectral lines represent about 39% (1/2.56) of the viewable data block. This requirement represents Shannon's Sampling requirement of two or greater samples per signal and anti-aliasing filter requirement. As the resolution is doubled, the blocksize and the acquisition time are doubled. For example, a resolution refinement of 1 to 1/4 Hz increase these values by a factor of 4, and a 1/10 Hz resolution increases them by 10. Once values are selected and the acquisition started, they remain fixed throughout the acquisition.

The FF version of an OT analysis continuously acquires data from the input signal and a reference speed signal with a fixed sampling frequency. This speed signal creates a reference between the rpm and time of each data point. Using this reference signal, a Fast Fourier Transform (FFT) divides the data block into multiple frequency spectrums. A waterfall plot is a common three-dimensional plot used to visualize the multiple spectrums at one time. Figure 3.2.1 illustrates a computational example containing a constant load AM signal with an 82nd carrier order along with two sidebands at the 16.4 and 147.6 orders.

This waterfall plot represents the frequency spectrum for a 190-758 output RPM (500-2000 input RPM) step-function with 37.8 RPM steps.

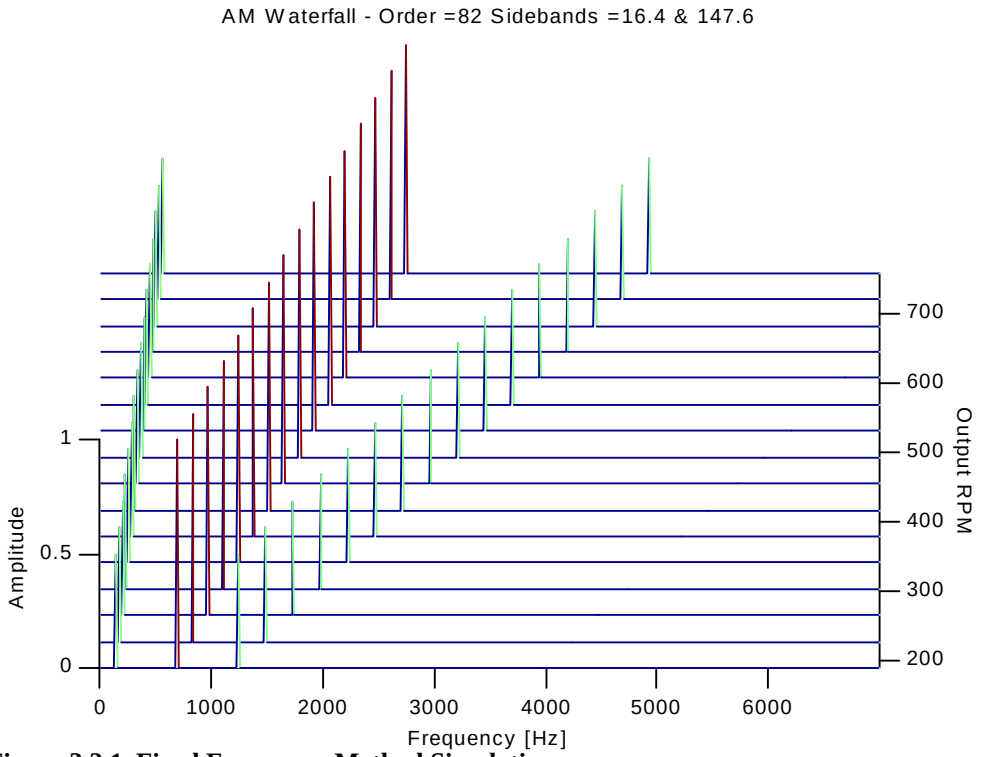

Figure 3.2.1. Fixed Frequency Method Simulation
A computer generated AM signal containing a carrier 82nd order with two sideband orders at 16.4 and 147.6 is stepped up through an output speed range of 190-758 RPM. (The speed range represents an input speed range from 500-2000 RPM of a Transfer Case with the 2.64 reduction planetary gear set.)

This method performs well for the step function where the RPM is held constant throughout the acquisition time of each step, but in reality, it is difficult to hold components at a constant RPM. In many applications, a constant or linear acceleration is needed, which requires a varying rotational speed during the DAQ process. The orders start at one frequency and end at another frequency at the end of the data block. The orders are now changing frequency during the DAQ time, and leakage[16] and smearing errors reduce their amplitudes. This movement causes the orders to be asynchronous within the DAQ time window, and the orders' energy leaks exponentially into the remaining spectral lines.

[16] McConnell, Kenneth G. Vibration Testing: Theory & Practice. New York, NY: John Wiley & Sons, Inc., 1995.

Unlike stationary asynchronous signals, the orders' amplitudes have an additional attenuation error when the leakage is smeared over more lines. As the spectral resolution increases, the orders will travel over more lines for the same ramp rate and further smear its amplitude.

3.2.2 Computed Order Tracking

With the increase of data acquisition speed, the Computed Order Tracking method was developed and patented by W. Potter. This technique acquires pseudo-synchronous data with minimal hardware. This technique uses a fixed sampling frequency DAQ board with a tachometer (tacho) signal to oversample and resample the data to generate a pseudo-synchronous data set.

The COT utilizes an encoder signal and the high sampling speed of the DAQ board to acquire a time-RPM reference signal. Since the analog channels are sampled at the same rate, the harmonics of interest have been at least 4 times oversampled in relation to requirement of Shannon's Sampling Theorem[17]. A constant angular acceleration assumption is applied to the data and represented in Eq. 3.2.3.1.

$$\theta(t) = b_0 + b_1 t + b_2 t^2 \tag{3.2.3.1}$$

Where θ is the shaft angle and b_0, b_1, and b_2 are the unknown coefficients. With the high sampled tacho signal, a relationship between the shaft position angle and the time of the sampled data is formulated. Three data points are needed to solve for the three unknown coefficients.

$$\theta(t_1) = 0$$
$$\theta(t_2) = \Delta\Phi$$
$$\theta(t_3) = 2\Delta\Phi$$

$$\begin{pmatrix} \theta(t_1) = 0 \\ \theta(t_2) = \Delta\Phi \\ \theta(t_3) = 2\Delta\Phi \end{pmatrix} = \begin{bmatrix} 1 & t_1 & {t_1}^2 \\ 1 & t_2 & {t_2}^2 \\ 1 & t_3 & {t_3}^2 \end{bmatrix} \begin{Bmatrix} b_0 \\ b_1 \\ b_2 \end{Bmatrix}$$

[17] Standard Mathematical Tables and Formulae. 30th ed. Ed. Daniel Zwillinger. Boca Raton: CRC Press, 1996. 535.

Where $\Delta\Phi$ represents the angle separating two consecutive encoder pulses (i.e. for a keyway $\Delta\Phi$ = 360° and for a 60 tooth tone wheel $\Delta\Phi$ = 6°). Once the *b* coefficients are known, Eq. 3.2.3.1 is rearranged to solve for the time at any shaft position and accordingly decimated or Resampled for the wanted shaft angle resolution (Eq. 3.2.3.2).

$$t = \frac{1}{2b_2}\left[\sqrt{4b_2(\theta - b_0) + b_1^{\,2}} - b_1\right] \tag{3.2.2.2}$$

Now, the amplitudes for the new times or shaft positions must be estimated. Cubic spline, piecewise cubic interpolations, and even simple linear interpolations are used to determine the best amplitude fit. The data has been rearranged into the synchronous sample or phase-locked format. A Fast Fourier Transform converts the data to the order domain.

Many errors could arise from the assumption and the data modeling. Low pulse encoders relative to the required shaft angle resolution, and the amplitude interpolation method both produce errors. The technique is more sensitive to the violation of the constant angular acceleration assumption with Non-linear acceleration and inaccurate tacho reading from a slow sampling frequency. The oversampling requirement becomes a limiting issue when high orders and fine resolutions are required.

3.2.3 Kalman Filters

A Kalman Filter is a narrow band pass digital filter used to track a specific waveform within multiple harmonic time signals. The filter solves both the Structural Equation (Eq. 3.2.3.1) representing a sine wave and the Data Equation (Eq.. 3.2.3.2) for the data block.

$$x(n) - c(n)x(n-1) + x(n-2) = \varepsilon(n) \tag{3.2.3.1}$$

$$y(n) = x(n) + \eta(n) \tag{3.2.3.2}$$

Where $c(n)=\cos(2\pi\omega\Delta t)$, $\varepsilon(n)$ is the nonhomogeneity term containing noise and other harmonics, and $\eta(n)$ also contains noise and other harmonics.

Since only three data points are needed to solve the pair of equations, a Least Square estimate manipulates the overdetermined system.

$$\begin{Bmatrix} 1 & -c(n) & 1 \\ & & r(n) \end{Bmatrix} \begin{Bmatrix} x(n-2) \\ x(n-1) \\ x(n) \end{Bmatrix} = \begin{bmatrix} \varepsilon(n) \\ r(n)(y(n)-\eta(n)) \end{bmatrix}$$

Where *r(n)* is a weighting function that influences the filter's shapes. A higher value relates to a sharper filter but the convergence is slower.

The slew rate limitation must be less than the $F_s/2T$ for a 1 Hz resolution. The speed signal must be sampled at a high rate and resampled (i.e. cubic spline) to acquire the arrival time to relate the signal to the order domain.

3.3 Synchronous Sampling

The SS method is analogous to the FS theory discussed at the beginning of Section 3.2.1. The underlying difference comes from the external sample clock requirement. Additional external hardware is used to generate an external sample clock signal. An optical encoder provides an output square wave to operate the A/D conversion of the DAQ computer board. If this encoder is mechanically locked to the rotating reference shaft, the input channels are sampled at constant shaft angles. The sampling rate is synchronized with the mechanics of the transfer case and is independent of any variations in shaft speed. The synchronous content of the gearmesh order is phase-locked to the beginning of the data block.

The same cut-off and sample requirements apply to the SS method, but these values pertain to orders instead of frequencies. The sampling order is determined by the pulses-per-revolution of the encoder. The resulting cut-off and maximum order are 50% and 39% respectively of the sampling order. With a blocksize of a power of two, the SS method utilizes a Fast Fourier Transform and directly transforms the data block into the order domain (Fig. 3.3.1). This system mimics the

basic FF method, but it removes the smearing and the estimate error associated with each of the methods mentioned above.

The disadvantages of this system are its difficulty to produce the appropriate external clock pulse for the A/D board and the speed of an anti-aliasing filter with a tracking or variable cut-off frequency. The optical encoder must be mechanically locked to the rotating system. This sensitive device is difficult to mount without subjecting it to the in-line torque loads.

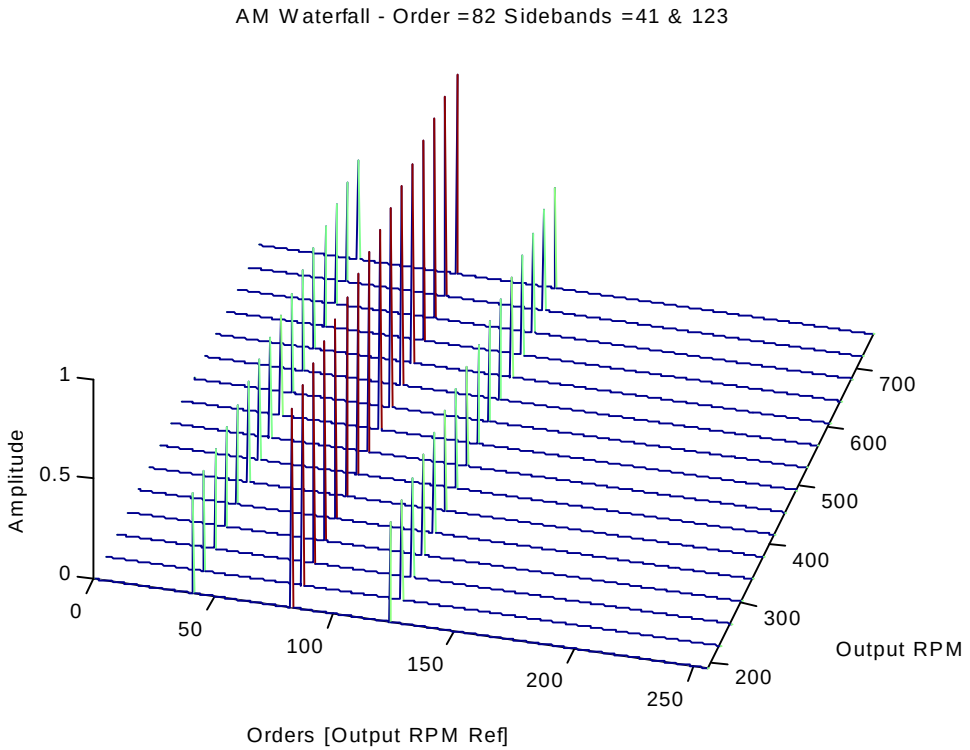

Figure 3.3.1. Synchronous Sampling Method – Simulation
A computer generated AM signal containing a carrier 82nd order with two sideband orders at 16.4 and 147.6 is stepped up through an output speed range of 190-758 RPM. (The speed range represents an input speed range from 500-2000 RPM of a Transfer Case with the 2.64 reduction planetary gear set.)

3.4 Averaging

Block averaging is a useful tool that is used by engineers to reduce the uncorrelated content and reveal the deterministic content of a data set. The Root-Mean-Square (RMS) averaging technique calculates the

RMS amplitude for the harmonic content (Eq. 3.4.1) and the variance for the noise content (Eq. 3.4.2).

$$A_{RMS} = \sqrt{\frac{\left(A_{peak}\right)^2}{2}} \tag{3.4.1}$$

$$S^2 = \frac{1}{N}\sum_{i}^{N}\left(x_i - \overline{x_i}\right)^2 \tag{3.4.2}$$

$$\overline{x_i} = 0$$

Where A_{peak} and A_{RMS} are the peak and RMS amplitudes of any harmonic content, N is the blocksize, and S^2 is the variance of the random or noise (x_i) content. These values are calculated with an AC coupling to assume mean zero data. The RMS average reduces the noise floor to the variance.

With the use of synchronous data blocks, a Synchronous or Vector Average (VA) is applied. The VA technique averages both the real and imaginary components of the signal. This more stringent technique converges the asynchronous and noise signals to zero while maintaining the synchronous components. Due to the phase variation of the asynchronous and noise signals, the expected value for the real and imaginary components are zero. Equation 3.4.3 represents the increase of signal-to-noise ratio[18] as a function of the number of vector averages.

$$S/n = 10 * Log10(n) \tag{3.4.3}$$

Table 3.4.1 lists the dB increase for the values of 3 orders-of-magnitude.

Table 3.4.1. Signal-to-Noise Ratio – Vector Averaging Effect

n	$n^{1/2}$	s/n [dB]
10	3.16…	10
100	10	20
1000	31.6…	30

Caution must be taken when applying the VA technique. The amplitude of an asynchronous order is attenuated from a leakage error, but unlike the RMS technique the VA furthers its decent into the noise floor.

[18] Shock and Vibration Handbook. 3rd ed. Ed. Syril Harris. New York: McGraw Hill, 1988.

Asynchronous orders contain a random phase variation relative to the beginning of the data block. Figures 3.4.1 & 3.4.2 show the phase variation for two different degrees of leakage. Variations of these were plotted (Fig. 3.4.3) for a number of different averages listed in Table 3.4.1. The scatter associated with the FS methods may add phase variations and decrease the synchronous content.

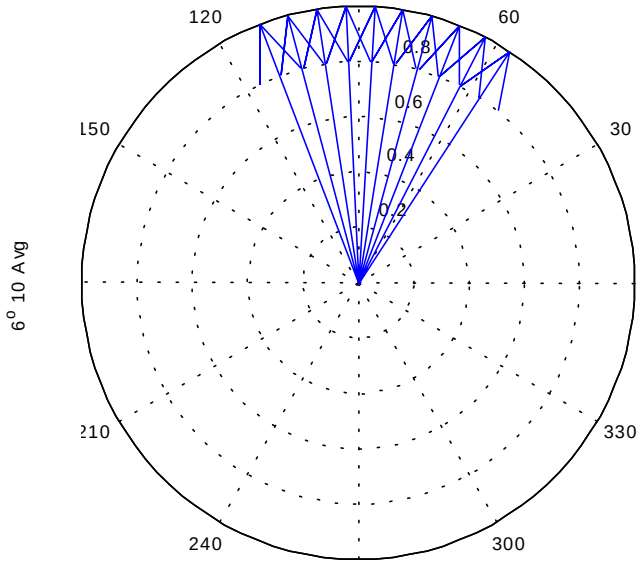

Figure 3.4.1. Vector Average – Small Frequency Difference
This represents an asynchronous signal slightly off from the acquisition time window. Only mild attenuation occurs.

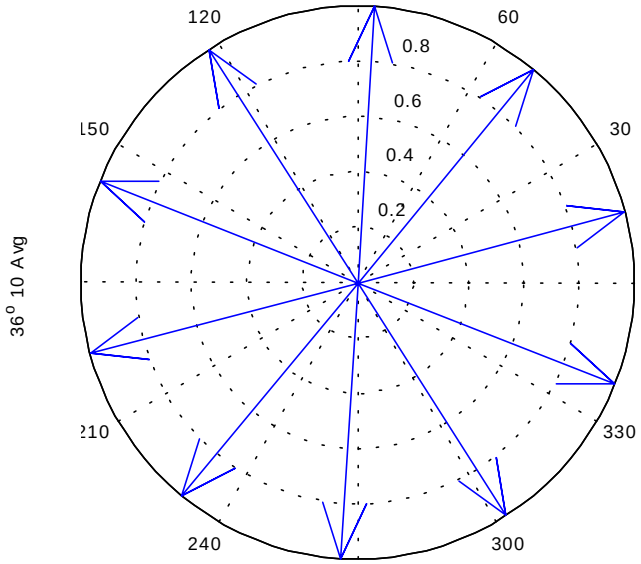

Figure 3.4.2. Vector Average – Phase Canceling
This is an asynchronous signal simulation of increased phase variation. This signal averages to zero.

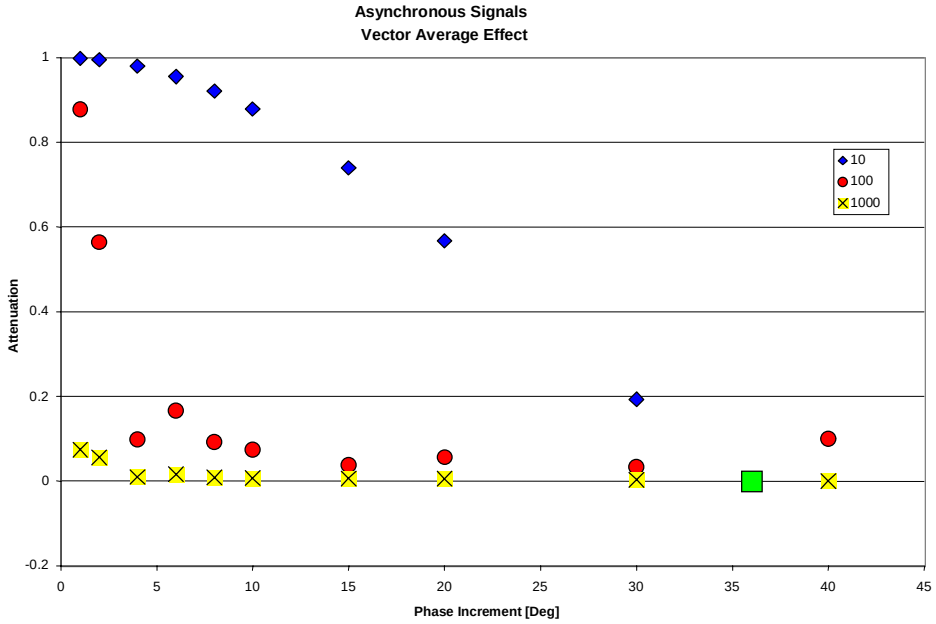

Figure 3.4.3. Vector Average – Sample Size and Phase Variation
The attenuation effects of asynchronous signals are plotted for eleven different phase variations. Three different runs were made for three different numbers of averages.

Vector Averaging is a useful tool that significantly lowers the noise floor below the RMS noise floor. This allows any hidden orders to rise

out of the noise. A better representation of the order domain advances the gear design process.

Chapter 4. Experimental Set-up

4.1 Experimental Set-up

The environment for this research was within a hemi-anechoic chamber capable of various speed and torque configurations (Fig. 4.1.1). The transfer case was bolted to a mounting fixture connected to an insulated base on the floor (Fig. 4.1.2). Three PC controlled electric motors drive the room's input and output propeller shafts.

Figure 4.1.1. Hemi-Anechoic Chamber – Exterior
The white room is the exterior of the hemi-anechoic (reflective floor) chamber, and the control station for the data acquisition and the chamber's motors. (Photo Courtesy of *Borg Warner Automotive - Powertrain Systems*, Sterling Heights, MI)

These shafts are connected to the transfer case's input, rear output, and front output. In-line torque cells and flexible couplings supported data

acquisition and motor control and isolated the transfer case setup from exterior rotary dynamics.

A PC with an internal two-channel data acquisition board sampled the speed and vibration of the transfer case. The acquisition board uses an external clock pulse from a digital optical encoder. The delicate nature of the encoder prevents it from being placed in-line with the high level torque of the propeller shafts. The belt and cog system (shown in Fig. 4.1.2) allows the encoder to be mechanically locked to the shaft speed while bypassing the torque.

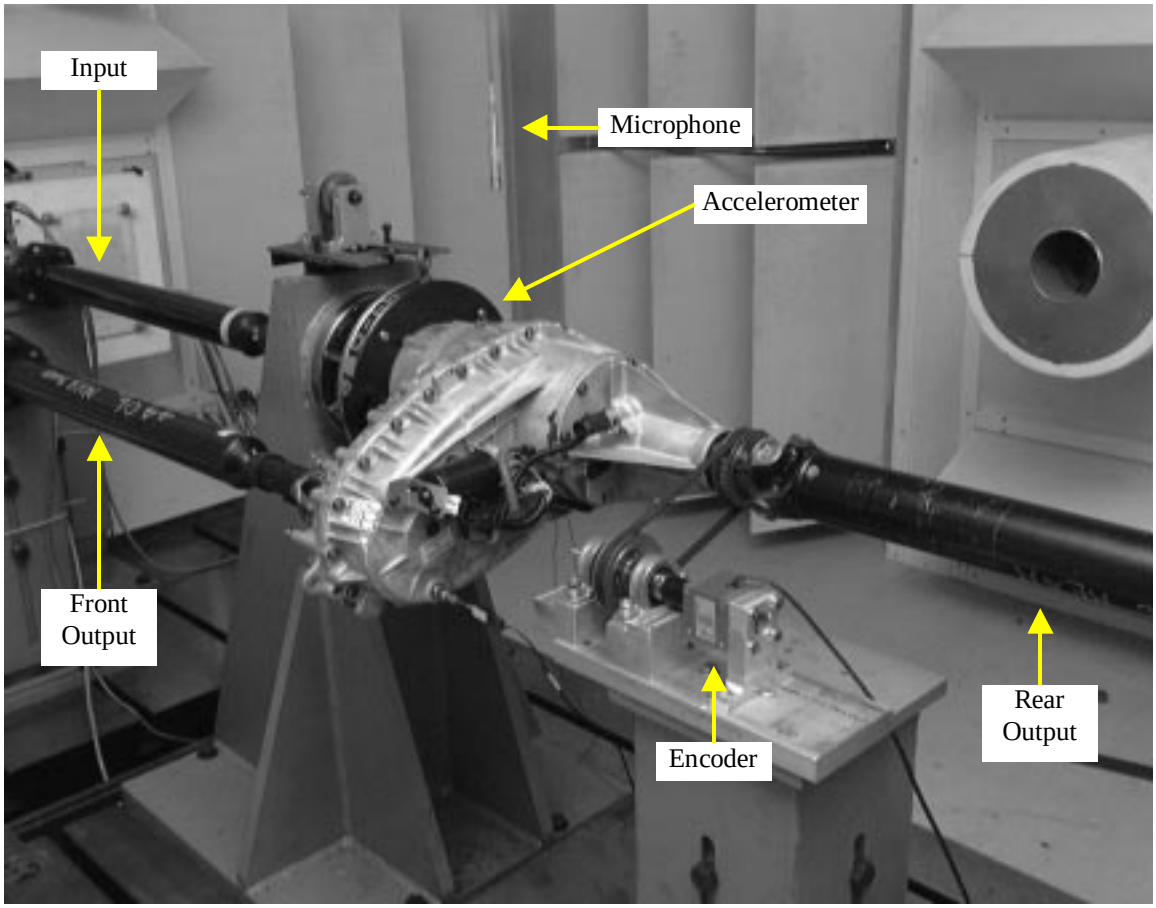

Figure 4.1.2. Hemi-Anechoic Chamber – Output Tracking
The rear view of the transfer case with the encoder belted off the rear output illustrates the test configuration used to track the output speed. The accelerometer is mounted at the top of the input casing with the microphone hanging above it (lowered for this illustration). (Photo Courtesy of *Borg Warner Automotive - Powertrain Systems*, Sterling Heights, MI)

This study used the rear output speed as the reference speed. An input speed reference causes the pinion/ring gearmesh order to be asynchronous as discussed earlier in section 2.3.

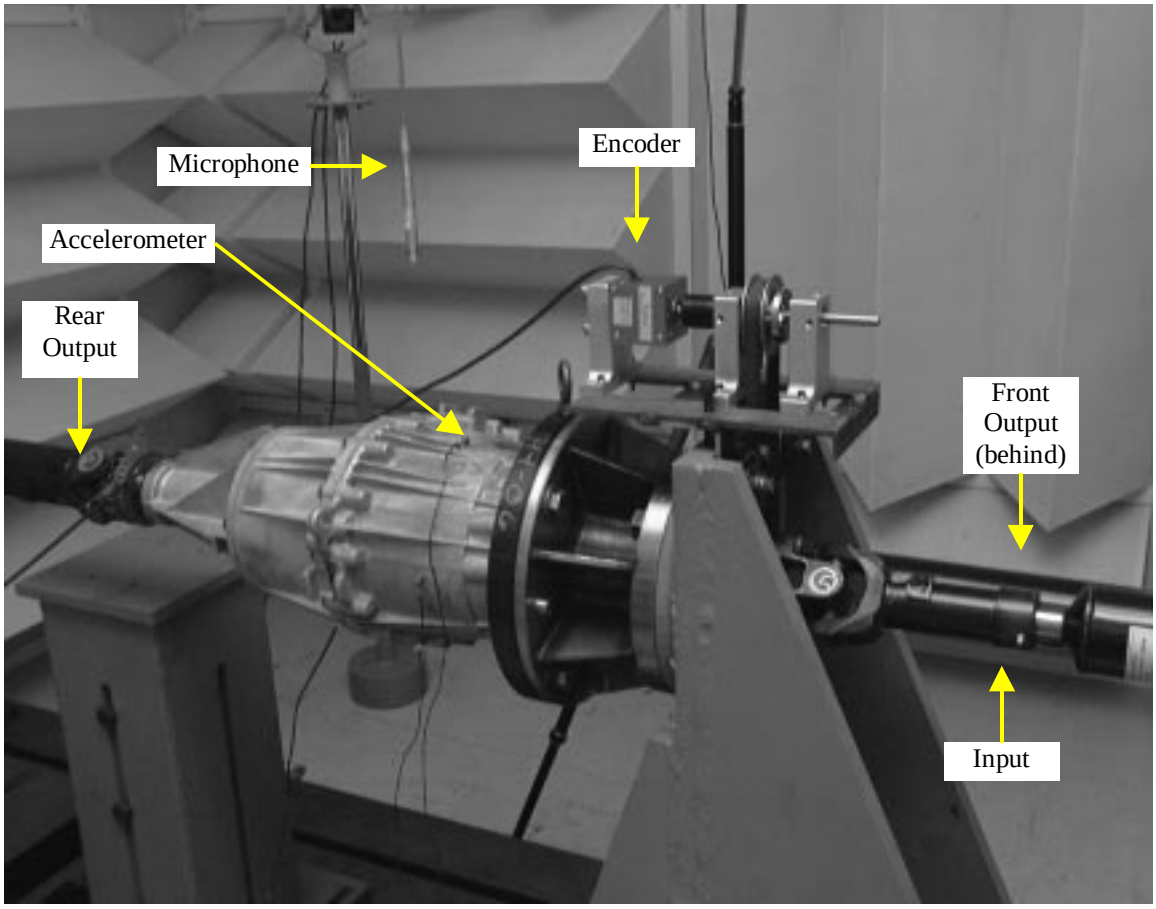

Figure 4.1.3. Hemi-Anechoic Chamber – Input Tracking
The side view of the transfer case with the encoder belted off the input illustrates the test configuration used to track the input speed. The accelerometer is mounted at the top of the input casing with the microphone hanging above it (lowered for this illustration). (Photo Courtesy of *Borg Warner Automotive - Powertrain Systems*, Sterling Heights, MI)

Calibration of all control and acquisition devices was conducted to assure the highest level of precision in the experiments.

4.2 Signal Conditioning

This encoder (Fig. 4.1.2 & 4.2.3) produces a 1024 p/rev and a 1 p/rev signal. The 1 p/rev is implemented to start the acquisition as a digital trigger. The 1024 p/rev is the external-sample-clock that implements the A/D conversion. Both of these signals exhibited a

ringing noise. This noise caused the acquisition hardware to trigger and sample at inappropriate times. This inaccuracy added phase variations within the synchronous content. Application of a VA significantly decreased the synchronous content. Although the source of this noise wasn't determined, a Schmitt trigger and a higher input voltage were both used on both encoder signals to remove this ringing noise and increase the frequency response of the wave form (Figure 4.2.1).

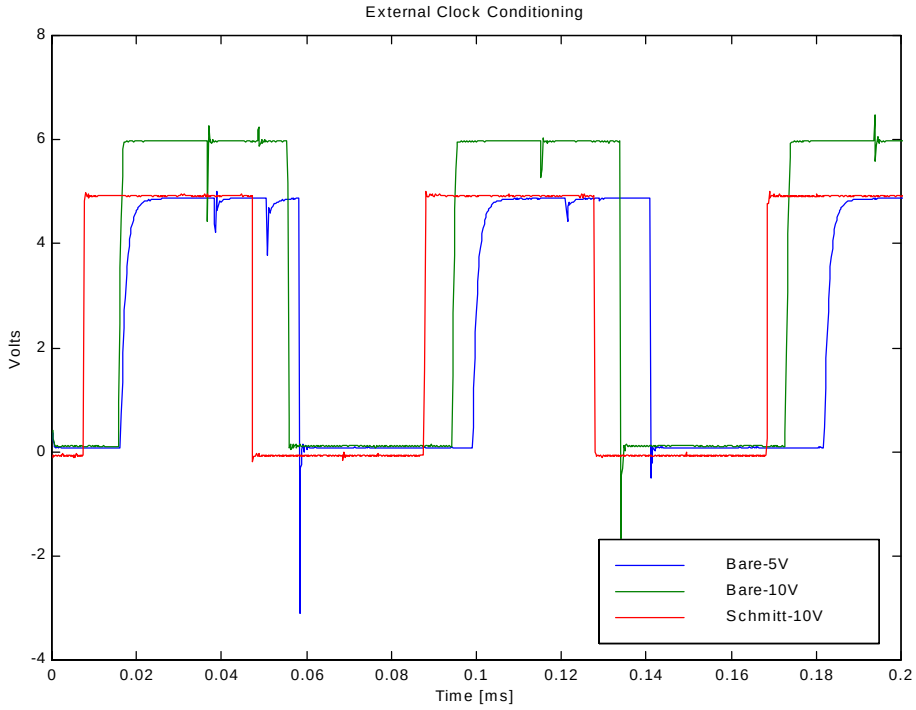

Figure 4.2.1. External-Sample-Clock – Signal Conditioning
The encoder signal shows the effects of the increased voltage to 10 volts and the Schmitt trigger. The 10 volts increases the frequency response of the signal, and the Schmitt trigger filters out the noise ring. (Waves are offset for viewing convenience.)

With the 1024-p/rev clock signal, the order spectrum produces a 400th order bandwidth. To reduce this bandwidth, a J-K Flip-Flop decreases this signal down to a 512 p/rev and a 256-p/rev signal. The 512-p/rev signal relates to a 200th order bandwidth that contains both fundamental gearmesh orders and the first harmonic of the pinion/ring gearmesh order.

Chapter 5. Synchronous Sampling of a SUV Transfer Case

5.1 Gear Set Order Evaluation

The SS of the SUV transfer case consists of the base configuration listed in Table 5.1.1 unless further noted in the following sections. The low range configuration of the transfer case forces the load path through the reduction planetary gear set (2.64:1).

Table 5.1.1. Transfer Case Configuration–Base Configuration

	Speed (RPM/Hz)	Load (in-lb./ft-LB)
Input	* 3000 / 50	606.6 / 50.5
Rear Output	1136.4 / 18.9	* 800 / 66.7
Front Output	1136.4 / 18.9	* 800 / 66.7

* Motor control input variables

The loads and speeds are held constant throughout the analysis. A typical speed signal contains only a minor variation of 0.01 Hz (0.6 RPM) and is assumed constant. The accelerometer position is fixed to the outside of the case near the input mounting (Fig. 4.1.2), and the microphone is hanging five feet directly above the accelerometer. This microphone distance is used to minimize the number of orders within the near field.

A 200th order bandwidth with a 0.125 order resolution contains the dominant orders of the transfer case. Figures 5.1.1 & 5.1.2 illustrate an extended bandwidth of 400 orders verifying this assumption for both the accelerometer and microphone respectively. The overshadowing 80th and 84th sideband orders lie near the pinion/ring fundamental gearmesh order (82nd) and its first harmonic (164th).

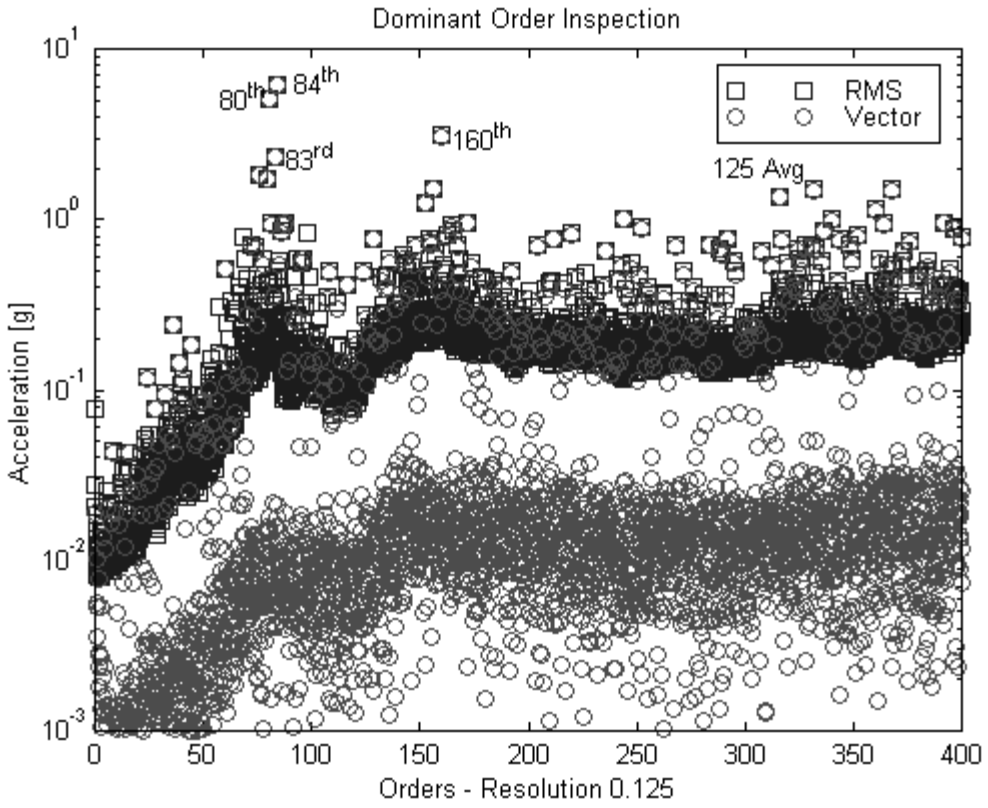

Figure 5.1.1. Order Spectrum – Bandwidth Verification
Accelerometer represents the dominant components at the 80th & 84th orders with comparable orders at the 83rd & 160th. A 200th order bandwidth covers the fundamental and 1st harmonic gearmesh orders and the dominant orders. (125 Avg.)

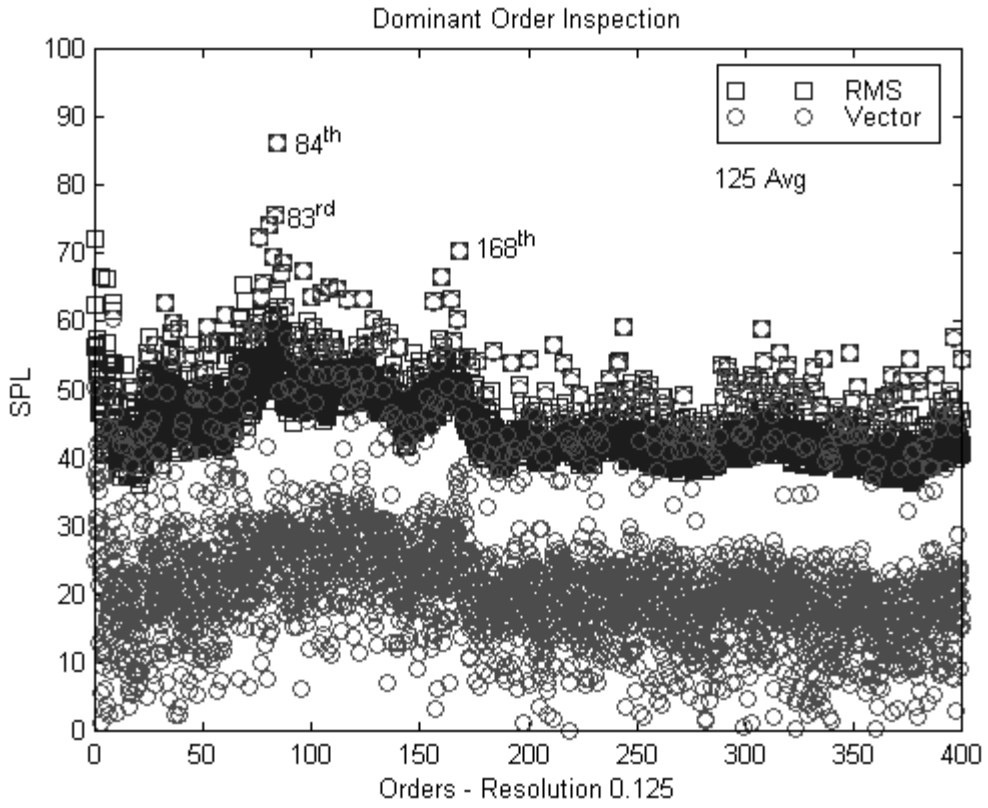

Figure 5.1.2. Order Spectrum – Bandwidth Verification
The microphone represents a dominant component at the 84th order with comparable orders at the 83rd & 168th. A 200th order bandwidth covers the fundamental and 1st harmonic gearmesh orders and the dominant orders. (125 Avg.)

Two main aspects should be noticed from the RMS and vector averaging techniques (125 averages). The vector averaged amplitudes lie on top of the RMS values for the theoretical synchronous orders like the 82nd gearmesh order. The fundamental and the first harmonic order of the gearmesh along with their sidebands clearly show strong synchronous content (Figure 5.1.3 & 5.1.4)

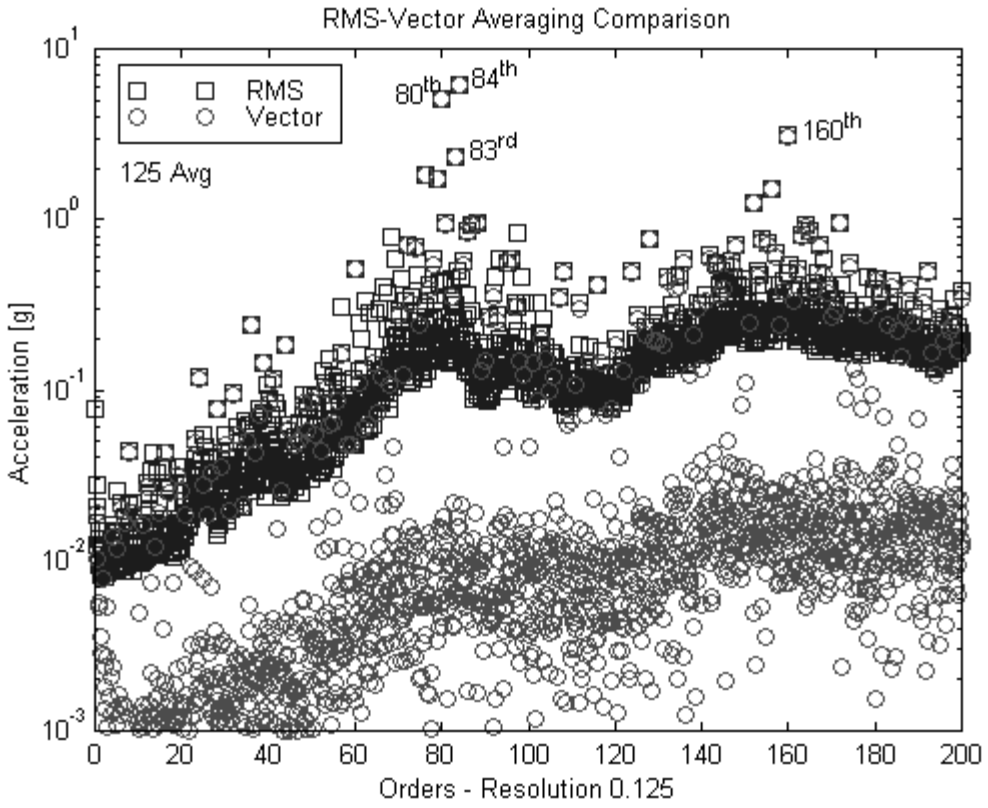

Figure 5.1.3. RMS and Vector Averaging – Acceleration
The acceleration represents relatively high values for the gearmesh and sideband orders. The Vector averaging technique (125 Avg.) has lowered the noise floor by approximately 21 dB.

Additionally, the VA significantly reduces the RMS noise floor. The asynchronous and noise content are lowered by approximately 20-21 dB. This corresponds to a S/N increase calculation (Eq. 3.4.3) for the 125 samples of 21 dB.

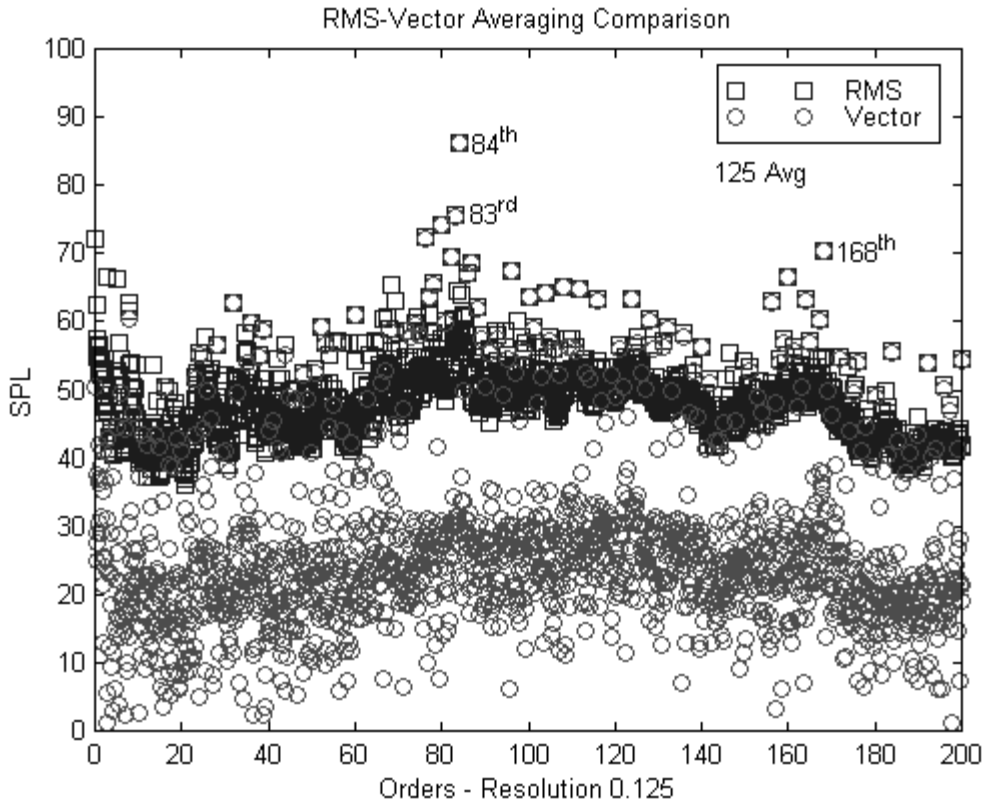

Figure 5.1.4. RMS and Vector Averaging – SPL
The sound pressure level represents relatively high values for the gearmesh and sideband orders. The vector averaging technique (125 Avg.) has lowered the noise floor by approximately 21 dB.

By substantially improving the S/N, many synchronous orders are revealed from the noise floor. Plotting the vectors for the fundamental gearmesh and the dominant sideband orders (Fig. 5.1.5) illustrates the phase-locked nature of the strong synchronous content. The orders with a relatively high RMS value and a decreasing VA value represent asynchronous orders. These orders show a phase variation that attenuates their amplitude (Fig. 5.1.6). The implementation of vector averaging improves the understanding of the order domain.

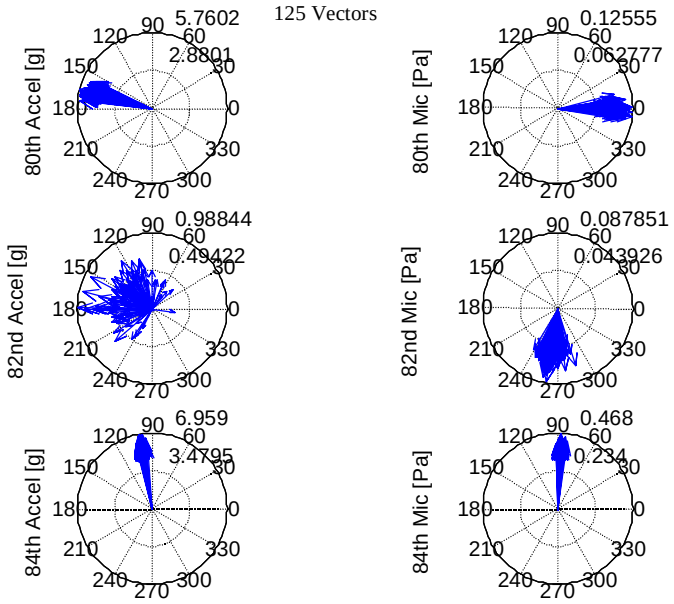

Figure 5.1.5. Order Vectors - Gearmesh and Sideband Orders
The vector representation of the acceleration (a,c,&e) and the pressure (b,d,&f) illustrates a synchronous nature of the gearmesh order (c&d) and the 80th and 84th sideband orders. (125 Vectors)

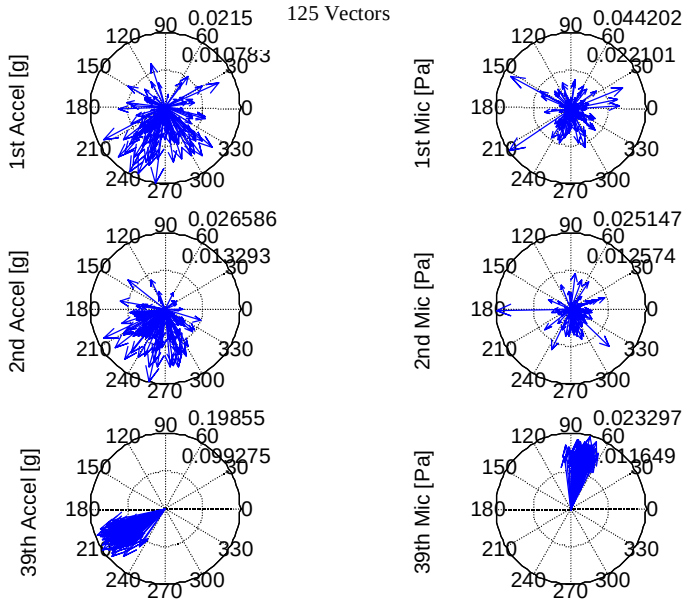

Figure 5.1.6. Order Vectors – Runout and Sprocket Orders
The vector representation of the acceleration (a,c,&e) and the pressure (b,d,&f) illustrates a synchronous sprocket order and asynchronous runout orders. (125 Vectors)

5.2 Method Comparison

A comparison analysis of the SS and COT method reveals noticeable differences in their order domain representation. For the base configuration, two different acquisition systems sampled the analog signals over the same 20 second span. The encoder signal is an external sample clock for the SS system and a reference speed signal for the FS system. The FS data set is resampled with a commercial system to 512 samples/rotation to mirror the similar SS data set. Both sets of data are then restructured with the same algorithm to present a 200th order bandwidth, a ¼ order resolution, and 97 RMS and vector averages. Both methods show the dominant sideband orders of the 82nd gearmesh order.

A vector comparison of the 80th, 82nd, and 84th orders depicts the error differences between the FS and SS methods. Since both data sets were taken over the same time, the same deterministic and noise contents reside in each system (Table 5.2.1).

Table 5.2.1. Synchronous Data Block Statistics

	Mean	Variance
SS-Accelerometer [g]	-3.5248	94.7201
SS-Microphone [Pa]	-0.05558	0.35788
RS-Accelerometer [g]	0.19271	85.39801
RS-Microphone [Pa]	-0.00088	0.16073

The COT method contains additional phase-noise content associated with the estimating error. With this error, the phase-noise varies between 40° and 60° (Fig. 5.2.1), which is an increase over the 10°-30° variation of the SS method (Fig. 5.2.2). The COT sampling method clearly increases the scatter into the order domain representation.

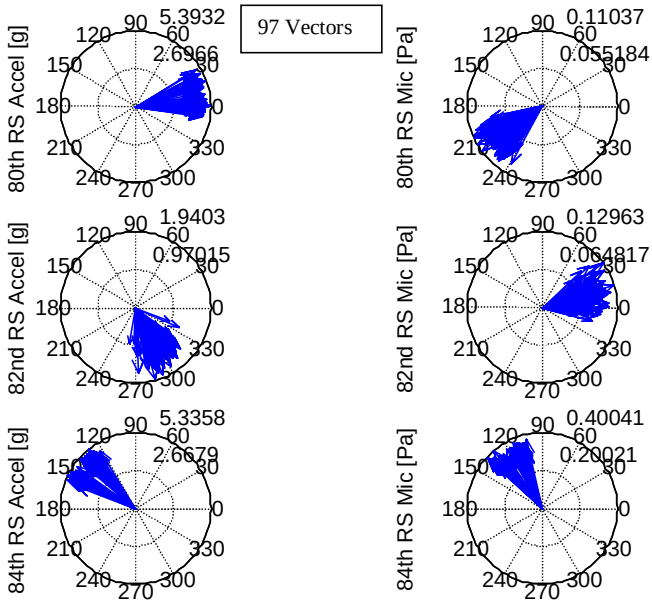

Figure 5.2.1. Vector Comparison – Resample
The gearmesh and sideband orders contain a greater phase variation between 40° and 60°. (97 Vectors)

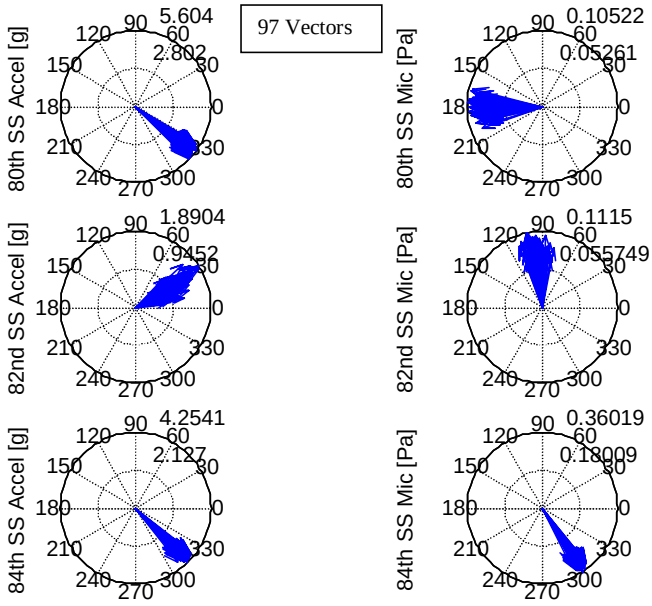

Figure 5.2.2. Vector Comparison – Synchronous Sampling
The gearmesh and sideband orders exhibit a low phase variation between 10° and 30°. (97 Vectors)

Relating this additional DSP error to the corresponding amplitude attenuation, RMS and vector averages are performed on both methods.

Inspection of a 20th order bandwidth around the 82nd gearmesh order illustrates (Fig. 5.2.3) a similar but inconsistent representation of the gearmesh and sideband orders by the COT. (Note the decibel scales.)

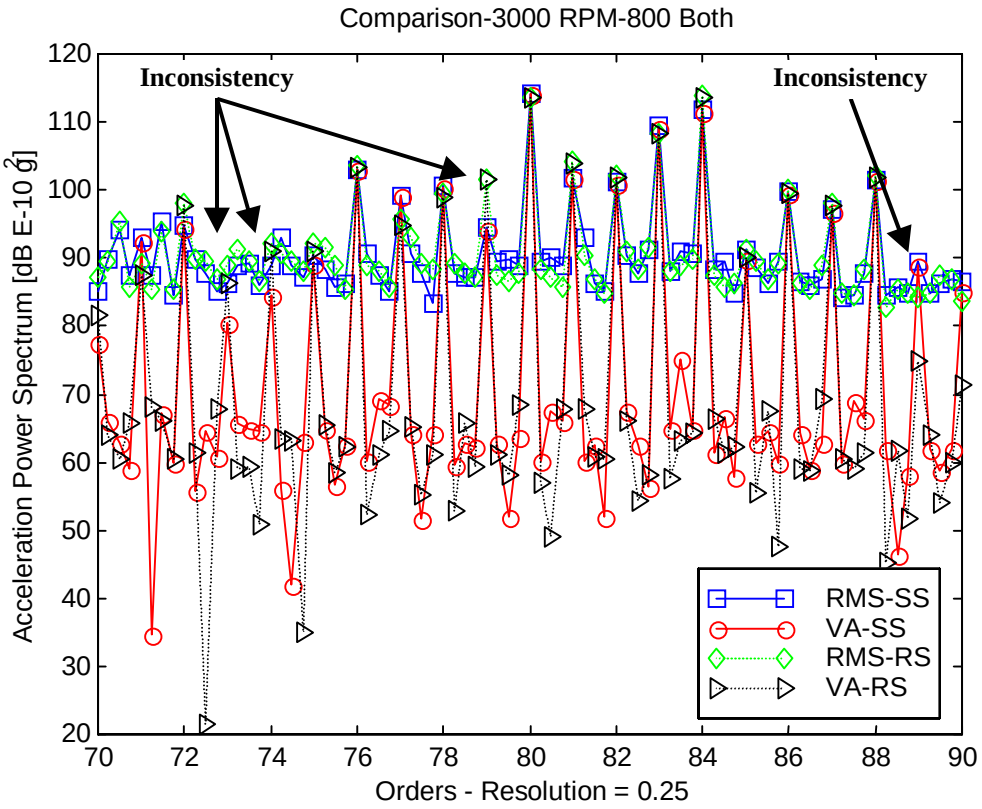

Figure 5.2.3 (a). SS-RS Amplitude Comparison
The acceleration (a) and the SPL (b) represent inconsistent relationships. (97 Avg.)

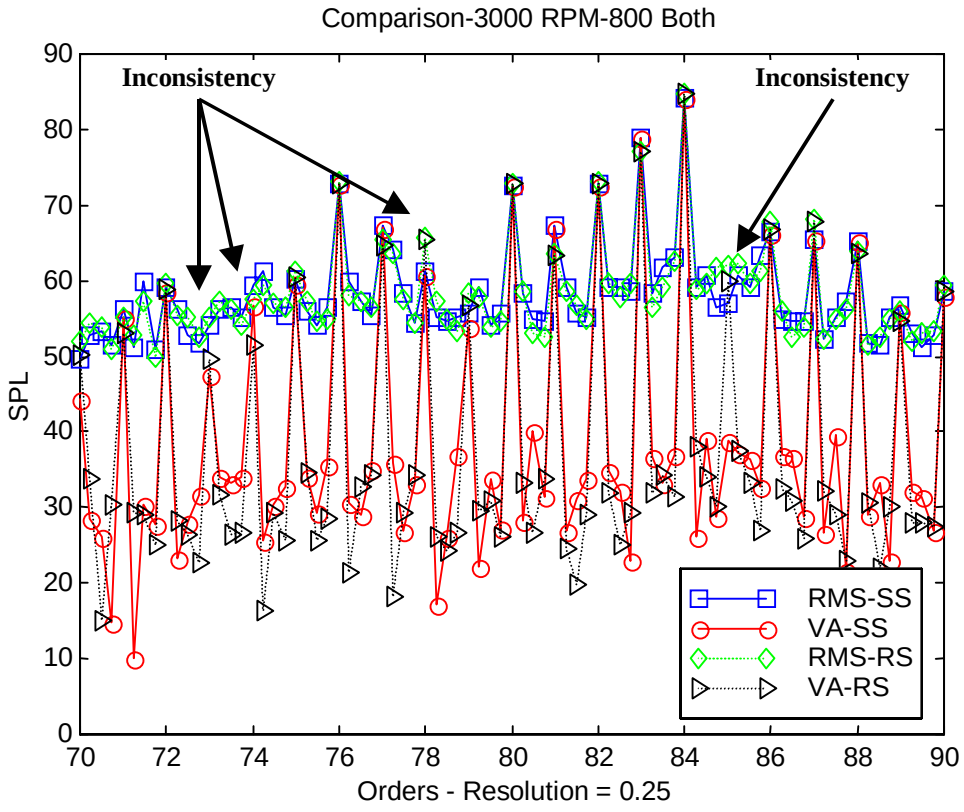

Figure 5.2.3 (b). SS-RS Amplitude Comparison
The acceleration (a) and the SPL (b) represent the inconsistent relationships. (97 Avg.)

The RMS and VA values of these amplitudes indicate an attenuation due to the additional phase variation. A greater concern comes from the inconsistency of the COT method at various orders throughout the order domain. Over-estimates of an order of magnitude are shown at the 73rd, 74th, & 79th orders where the SS resembles an asynchronous nature. In contrast, the COT method severely attenuates the 89th order that the SS method represents as a synchronous order. The above conflicts represent the benefits of implementing the SS method to improve the order domain representation.

5.3 Load Evaluation

To further the gear set knowledge, a series of experiments are conducted with the SS method to evaluate the loading effects of the transfer case. By vector averaging the synchronized data blocks of the

SS method, this load evaluation reveals an improved understanding of the gear set characteristics. Three different motor configurations are applied with five different loads at a constant RPM. As in common application of low-range, both the front and the rear outputs are carrying load in the transfer case (Table 5.3.1).

Table 5.3.1. Load Evaluation – Both Motors

	Speed (RPM/Hz)	Load (in-lb./ft-lb)				
Input	3000 / 50	606.6 / 50.5	454.5 / 37.9	303.3 / 25.3	151.5 / 12.6	0
Front Output	1136.4 / 18.9	800 / 66.7	600 / 50	400 / 33.3	200 / 16.7	0
Rear Output	1136.4 / 18.9	800 / 66.7	600 / 50	400 / 33.3	200 / 16.7	0

Individually loading the transfer case with the front output (Table 5.3.2) represent the analysis of a "broken back" design. A direct coupling is evaluated from the individual loading of the rear output (Table 5.3.3). One zero-load case is implemented to fill each load array.

Table 5.3.2. Load Evaluation – Front Motor

	Speed (RPM/Hz)	Load (in-lb./ft-lb)				
Input	3000 / 50	606.6 / 50.5	454.5 / 37.9	303.3 / 25.3	151.5 / 12.6	0
Front Output	1136.4 / 18.9	1600 / 133.3	1200 / 100	800 / 66.7	400 / 33.3	0
Rear Output	1136.4 / 18.9	0	0	0	0	0

Table 5.3.3. Load Evaluation – Rear Motor

	Speed (RPM/Hz)	Load (in-lb./ft-lb)				
Input	3000 / 50	606.6 / 50.5	454.5 / 37.9	303.3 / 25.3	151.5 / 12.6	0
Front Output	1136.4 / 18.9	0	0	0	0	0
Rear Output	1136.4 / 18.9	1600 / 133.3	1200 / 100	800 / 66.7	400 / 33.3	0

The gearmesh (82^{nd}) and the dominant sideband (80^{th} & 84^{th}) orders are tracked for the different load ranges. These loads have little influence on the gearmesh amplitude, but the sidebands show a strong relationship. Although the 84^{th} order exhibits a strong influence by the acceleration (Fig. 5.3.1) and the SPL (Fig. 5.3.2), the 80^{th} order only represents this influence in the acceleration.

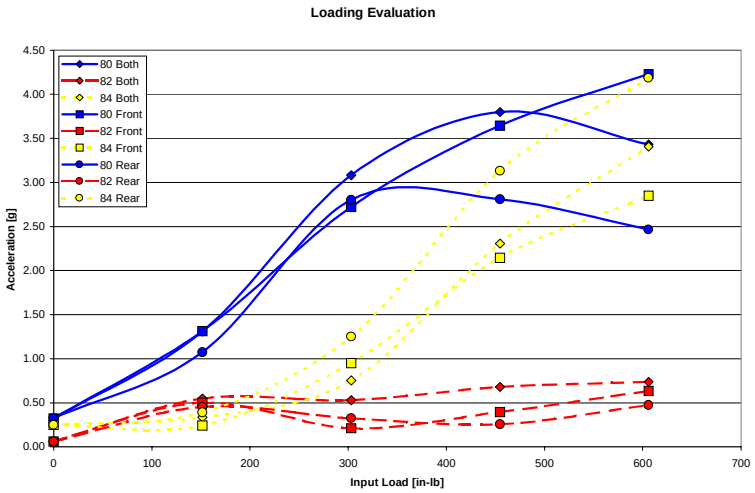

Figure 5.3.1. Loading Evaluation – Acceleration
The 84th order increases in acceleration with increasing load. The 80th order shows a decreasing effect at the higher loads, and the 82nd order shows little effect.

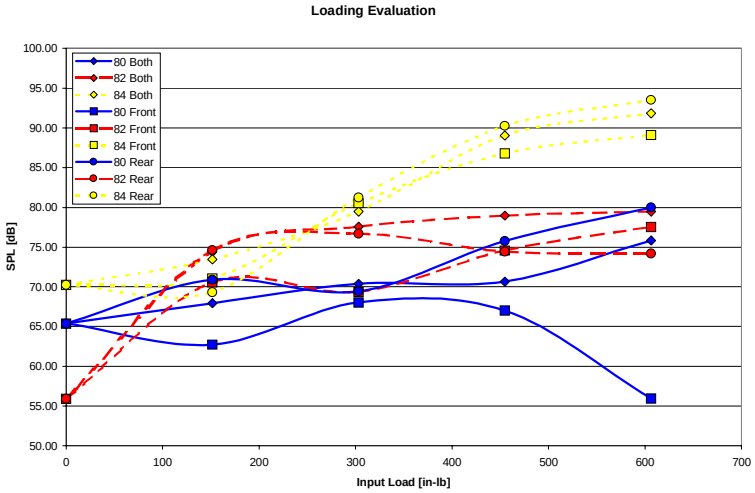

Figure 5.3.2. Loading Evaluation – SPL
The 84th order represents the same increasing form as for the acceleration. The 80th and 82nd orders oscillate 10 dB below the 84th.

Each of the three load cases depicts a general trend concerning each order. This trend is represented in Figures 5.3.1 & 5.3.2 by the line color or style. Normalizing the amplitudes by their maximum values allows the trend of the lower 82nd order to be compared with the sideband orders (Fig. 5.3.3). The origin of this trend is unknown, but merits further investigation.

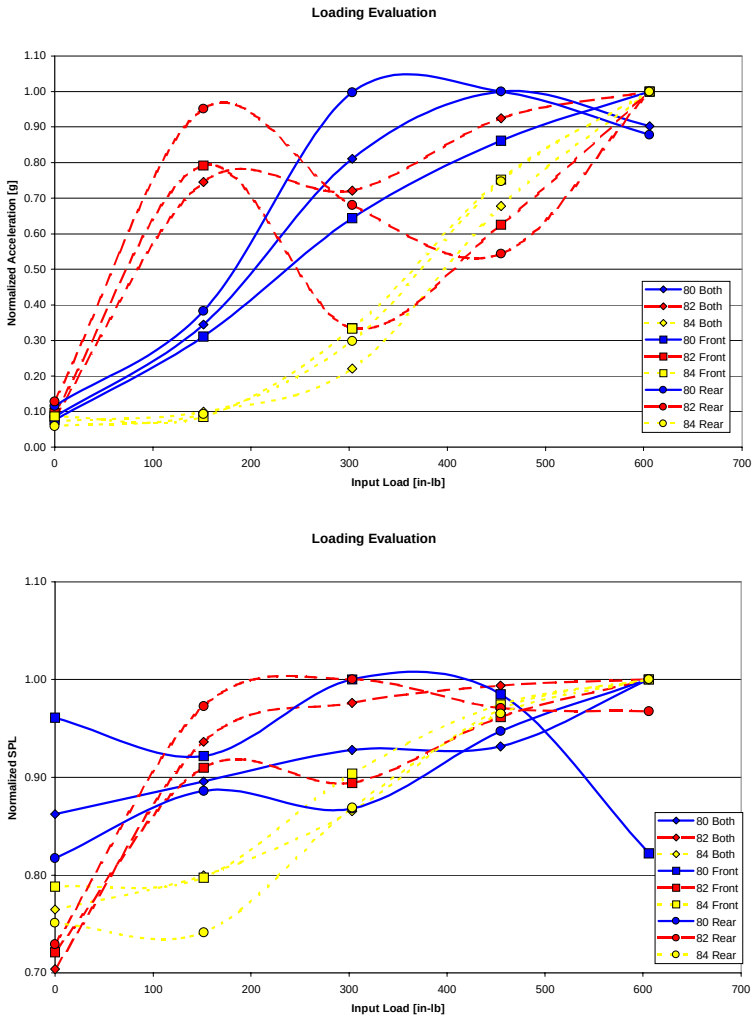

Figure 5.3.3. Load Evaluation – Normalized Acceleration and SPL
Each order displays the general trend for each motor configuration. For each order, this trend is represented by the color and line style.

5.4 Speed Evaluation

The SS method is also used to evaluate the transfer case gear set at different input shaft speeds. Vector averaging of the synchronous data blocks improves the representation of this speed evaluation in the order domain. This analysis consists of the base configuration with an input speed step–function. This function steps through 1000-3000 RPM range with 100 RPM increments. The speed is held constant throughout the time of the acquisition.

For this speed range, common waterfall plots illustrate the increase in the acceleration (Fig. 5.4.1) and pressure (Fig. 5.4.2) relative to the rotating speed for the order domain. Inspection analysis of these plots, reveals that the surrounding orders of the pinion/ring gearmesh and its first harmonic are the dominant orders throughout the order domain.

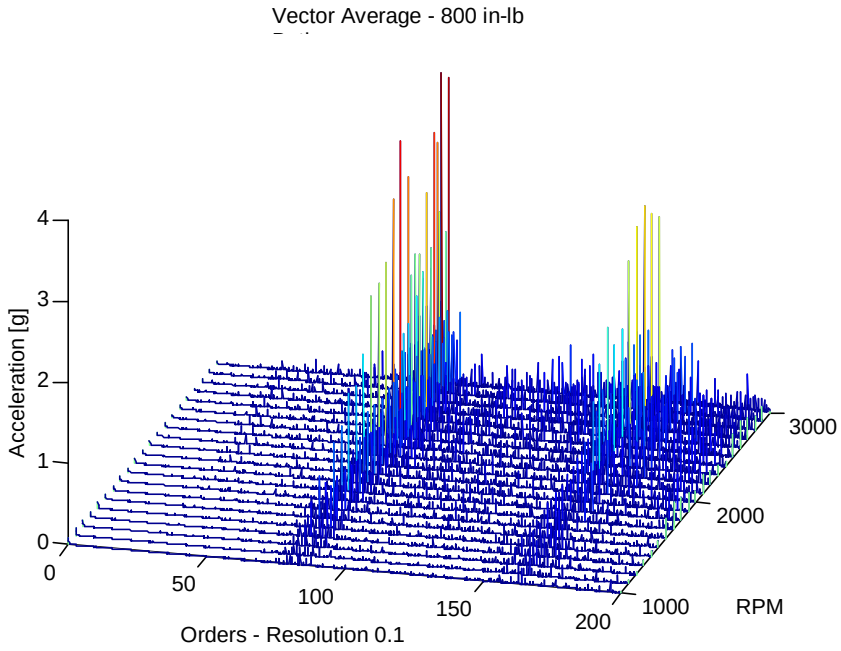

Figure 5.4.1. Waterfall – Acceleration
The 80th & 84th orders dominate the order spectrum with a noticeable contribution at the 160th order. These orders are substantially higher than their relative fundamental gearmesh and 1st harmonic orders. These orders oscillate with increasing shaft speed.

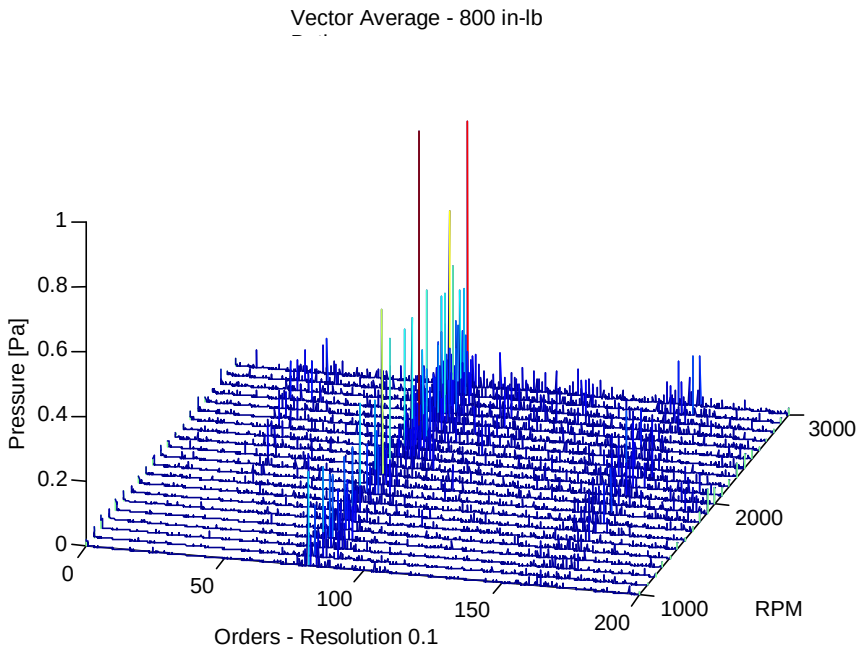

Figure 5.4.2. Waterfall – Pressure
The 80th & 84th sideband orders dominate order domain. These orders oscillate in amplitude with increasing shaft speed.

For a more in-depth look at these dominant orders (80th, 82nd, & 84th), 2D order plots track their amplitude throughout the rpm range. The acceleration values for these orders show a similar stepping trend at the lower speed along with an oscillating trend at the upper speeds (Fig. 5.4.3).

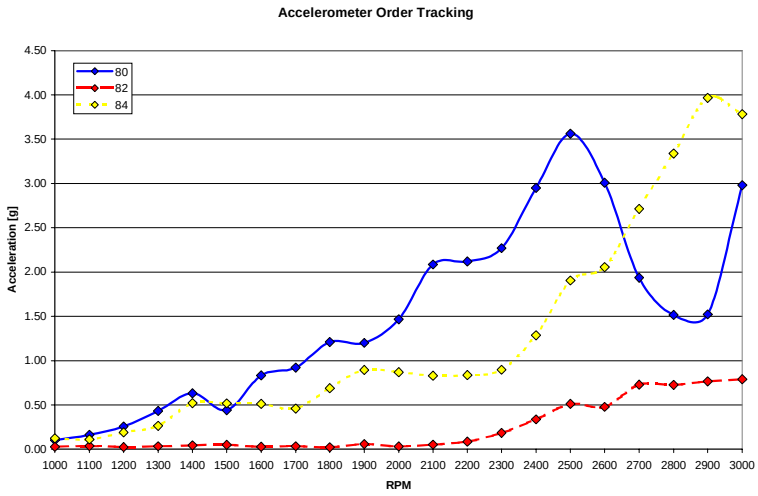

Figure 5.4.3. Order Tracking – Acceleration
The orders step up and then oscillate at the higher shaft speed. The 80th, 82nd, and 84th orders have similar trends with a respective lag between them.

In addition to their similar form, the 80th, 82nd, and 84th orders contain a relative lag between them. The pressure and the SPL (Fig. 5.4.4) values for these orders also show similar forms in relation to each other. Although these microphone values have a higher frequency of oscillation then the accelerometer values, the same relative lag occurs. The origin of these trends are unknown and beyond the scope of this research.

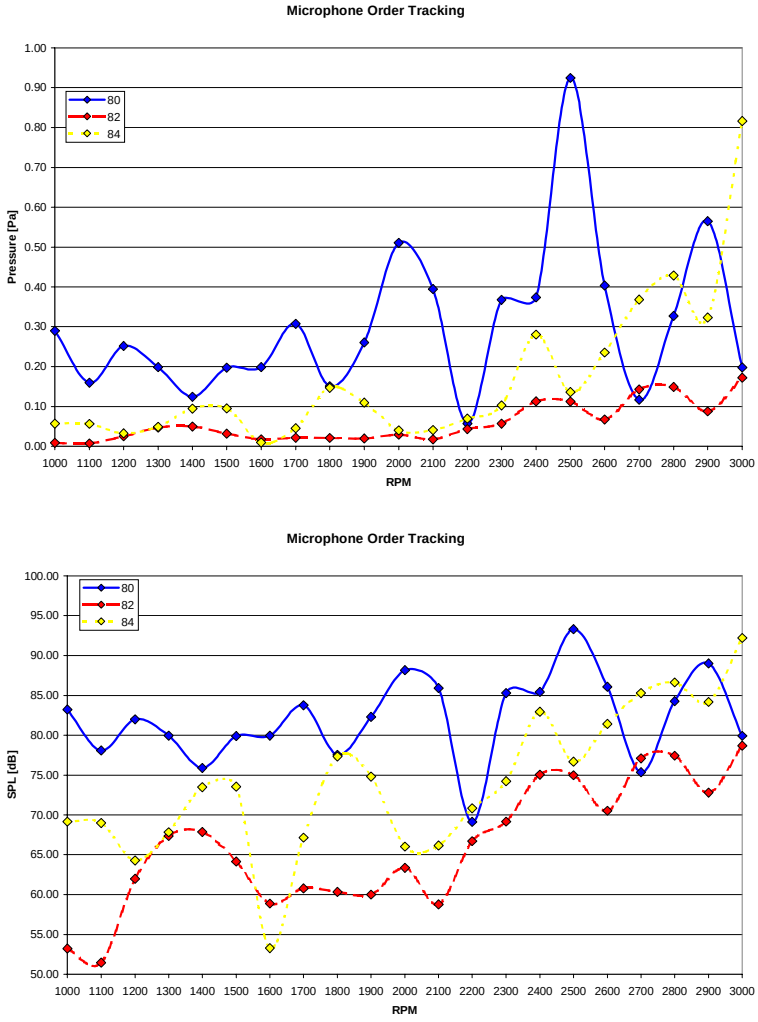

Figure 5.4.4. Order Tracking – Pressure and SPL
The orders oscillate throughout the speed range. The 80th, 82nd, and 84th orders have similar trends with a respective lag between them.

Chapter 6. Conclusions

6.1 Conclusions

The following details the conclusions drawn from the results of the Synchronous Sampling of a SUV transfer case. Specifically included are discussion of the gearmesh and dominant sideband orders; the affects of vector averaging on these orders; a comparison of the Synchronous Sampling and the COT method; and evaluation of the effects of load and speed on the transfer case.

Applying this SS method to the SUV transfer case resulted in an order domain dominated by the sidebands (80^{th} & 84^{th}) of the pinion/ring gearmesh order (82^{nd}). The use of vector averaging removed the asynchronous and noise content from this synchronous data set. Vector averaging (125 averages) enhanced this order domain representation by increasing the S/N by 21 dB. (This increase agreed with the calculated prediction for this sample size.) The substantial decrease in the noise floor revealed the orders that were previously hidden in the RMS noise. This improved representation of the order domain will further the gear design process. Therefore, the SS method is a valid and a useful tool to evaluate order content in a rotary dynamic system.

While comparing this system with a commercial FS system, an additional 30° of phase-noise was added by the COT estimating error. With this error, the COT inconsistently estimated the synchronous and asynchronous orders. This inconsistency may lead to misinterpretations.

While tracking the 80^{th}, 82^{nd}, and 84^{th} orders with the SS system, five different loads were applied for a constant shaft speed. These loads were applied individually and simultaneously to the rear and front outputs. The 82^{nd} gearmesh order remained unaffected by the increase in shaft load. The 84^{th} sideband order showed an increasing trend in the acceleration and pressure with the increase in shaft load. The 80^{th}

sideband order illustrated an oscillator characteristic as a function of the motor configuration. The origins of these trends are unknown, but they merit further investigation.

The SS method was also used to evaluate the transfer case gear set at different shaft speeds. These speeds are applied incrementally throughout the 1000-3000 RPM range. Throughout this range, the 82nd gearmesh order and the dominant 80th and 84th sideband orders illustrated similar order tracking curves with a relative lag between them. Further investigation into the origin of these curves would advance the sideband design process.

The Synchronous Sampling method as applied to the rotary dynamics of the SUV transfer case was shown to be useful tool. The additional application of vector averaging significantly improved the signal-to-noise ratio and the understanding of the order domain. Using these methods for evaluation of load and speed effects, revealed noticeable trends, warranting further research. Therefore, the research detailed here has provided important advancements in the data acquisition process and the general knowledge of the planetary gear set within the transfer case.

6.2 Suggestions for Future Research

Advancements of this work can be made in many facets of both the data acquisition system and the knowledge of the planetary gear set. The SS data acquisition system should be applied to run-up experiments for further comparisons with the COT method. Along with this system improvement, an increase in the data acquisition channels will increase the correlation capabilities of the acceleration, SPL, speed, and input loading for both the steady state and variable speed studies. These improvements also expand the correlative possibilities between the experimental data of geometric gear flaws and the theoretical modulation

models. The repeatability of the above experiments should also be addressed.

Vita

Chad Fair was born in 1972 in Three Rivers, Michigan. He graduated from Michigan Technological University in February 1996 with a Bachelor of Science in Mechanical Engineering. He worked for the Powertrain Systems Division of Borg Warner Automotive from February until August in 1996. In August 1996, he began pursuing a Masters of Science degree in Mechanical Engineering at Virginia Polytechnic Institute and State University.